VIRULENCE
2026, VOL. 17, NO. 1, 2636341
https://doi.org/10.1080/21505594.2026.2636341

Taylor & Francis
Taylor & Francis Group

VIRAL PATHOGENESIS

A hepcidin homolog from *Lateolabrax japonicus* inhibits the infection of Anguillid herpesvirus 1 by interacting with the viral envelope protein ORF51

Yingyi Duan[a,b*], Jun-Qing Ge[b*], Xin-Zhan Meng[a*], Fangyi Chen[a,c,d], and Ke-Jian Wang [a,c,d]

[a]State Key Laboratory of Marine Environmental Science, College of Ocean and Earth Sciences, Xiamen University, Xiamen, China; [b]Institute of Biotechnology, Fujian Academy of Agricultural Sciences, Fuzhou, China; [c]State-Province Joint Engineering Laboratory of Marine Bioproducts and Technology, College of Ocean and Earth Sciences, Xiamen University, Xiamen, China; [d]Marine Biological Antimicrobial Peptide Industry Research Institute, Fujian Ocean Innovation Center, Xiamen, China

ABSTRACT

Frequent outbreaks of eel "mucus sloughing and hemorrhagic septicemia disease" caused by Anguillid herpesvirus 1 (AngHV) are a major epidemic in both wild and farmed eels. This virus has garnered global attention due to heavy losses on eel farms and the lack of protective vaccines or effective drugs, highlighting the urgent need for potent antiviral agents. In this study, we revealed a hepcidin homolog LJ-hep2 from Japanese seabass (*Lateolabrax japonicus*) can bind to AngHV and impede viral entry into cells. LJ-hep2 could directly destroy the viral envelope and showed a higher anti-AngHV activity than AA-hep (a hepcidin homolog cloned from *Anguilla anguilla*). It was found that the destruction of viral structure by LJ-hep2 was related to the binding of the peptide to AngHV envelope protein ORF51, and the two amino acid residues at the N-terminus of the peptide (lysine and phenylalanine) might play a key role. Comparative antiviral experiments with mutated LJ-hep2 (LJ-hep2$_{A4A5}$) and multi-species hepcidin further confirmed this finding and demonstrated that these two amino acids were indispensable in the inhibition of AngHV infection by LJ-hep2. In an established eel immersion infection model, LJ-hep2 treatment reduced viral accumulation in tissues, inhibited horizontal transmission, alleviated skin lesions, and improved eel survival. Taken together, this study suggests that LJ-hep2 could inhibit AngHV infection *in vitro* and *in vivo*, and identify ORF51 as a potential target for the development of anti-AngHV drugs.

ARTICLE HISTORY
Received 25 September 2024
Revised 17 February 2026
Accepted 19 February 2026

KEYWORDS
Antimicrobial peptide; hepcidin; anguillid herpesvirus 1; antiviral activity; envelope protein ORF51

Introduction

Eels (*Anguilla* spp.) are widely farmed globally, with 47 countries engaged in eel production, yielding around 275,000 metric tons valued at approximately 2.5×10^9 USD [1]. However, viral infections have severely hampered the development of eel farming [2] and are considered to be the main cause of the worldwide decline in eel populations [3]. Anguillid herpesvirus 1 (AngHV, genus *Cyprinivirus*) is an enveloped double-stranded DNA virus that poses a serious threat to eels [4,5]. The virus is highly contagious and spreads horizontally, mainly through waterborne transmission. It is transmitted not only within farm ponds but also through water sources, transport vehicles, people, and other means, thus facilitating the spread of the virus to other eel farms [6–8]. In China, outbreaks of mucus sloughing and hemorrhagic septicemia disease occur annually in farmed eels, with mortality rates as high as 30%, resulting in substantial economic losses [9,10]. Currently, methods of controlling this disease mainly include lowering the breeding water temperature, minimizing or halting feeding, and administering some surfactants [11]. However, the effectiveness of these measures remains inadequate [12], emphasizing the urgent need to develop antiviral agents that can serve as prophylactic or therapeutic agents against AngHV.

Antimicrobial peptides (AMPs) have received extensive attention from the scientific community due to their great potential in antiviral activity [13]. As an important component of innate immunity, AMPs play a critical role in clearing pathogens and modulating host immune responses [14–16]. Marine sources account for half of the total global biodiversity and are the largest source of supply of natural peptides. To adapt to the harsh marine environment, these peptides undergo structural modifications that result in the acquisition of features that can maintain biological properties against pathogens [17]. Therefore, marine-derived peptides have been regarded as potential candidates for anti-infective drugs [18,19]. Moreover, in terms of drug-like properties, peptides possess similar

CONTACT Fangyi Chen chenfangyi@xmu.edu.cn; Ke-Jian Wang wkjian@xmu.edu.cn
*These authors contributed equally to this work.
Supplemental data for this article can be accessed online at https://doi.org/10.1080/21505594.2026.2636341.

characteristics to antibodies and small molecules and act as a bridge between antibody drugs and small molecules. They can be converted into peptidomimetics with small-molecule properties while retaining some of the amino acids and binding specificity, maintaining protein- or biotechnology-based drug characteristics [20]. Given their superior efficacy, high selectivity, and low drug resistance potential, the pharmaceutical industry is increasingly focusing on the development of peptide drugs [17,21,22].

Our previous studies identified three marine-derived AMPs: LJ-hepcidin2$_{66–86}$ (LJ-hep2), which is the mature peptide of hepcidin2 from Japanese seabass (*Lateolabrax japonicus*) [23], Scyampcin$_{44–63}$ from the mud crab (*Scylla paramamosain*) [24], and Moronecidin$_{23–44}$ from the rockfish (*Sebastiscus marmoratus*) [25]. Although these peptides exhibited excellent antibacterial and antifungal activity, limited information was available regarding their antiviral effects. Notably, hepcidin, an important classical AMP peptide, is widely present in teleosts [26,27]. Recently, several fish hepcidins have been reported to possess antiviral activity, such as protection of spotted grouper (*Epinephelus coioides*) larvae from Nervous necrosis virus (NNV) infection [28] and improved the survival of Chinook salmon embryo (CHSE)-214 cells infected with Infectious Pancreatic Necrosis Virus (IPNV) [29]. However, it is still unknown whether hepcidin can inhibit AngHV infection.

In this study, we cloned and identified a hepcidin gene (AA-hepcidin) from the European eel (*Anguilla anguilla*). Its derived peptide, AA-hepcidin$_{69–89}$ (AA-hep), together with the three aforementioned AMPs (LJ-hep2, Scyampcin$_{44–63}$, and Moronecidin$_{23–44}$) was subsequently subjected to an anti-AngHV screening assay. *In vitro* assays were employed to evaluate the potential anti-AngHV activity and toxicity of the four AMPs. Further investigations included assessing their effects on viral entry using fluorescence microscopy and flow cytometry, evaluating their effects on virion integrity through transmission electron microscopy (TEM) and DNase digestion assay, and exploring differences in their binding to viral envelope proteins through *in-silico* approaches and pull-down analysis. The truncation of AMP allowed exploration of the antiviral activity of different regions of AMP, thereby identifying the key regions of AMP with anti-AngHV activity. The key sites for the antiviral activity of AMP were explored through an amino acid mutation experiment. Based on the *in vitro* antiviral results, we selected the most effective AMP for *in vivo* validation of antiviral activity through viral-immersed infection and horizontal transmission models. Parameters, such as infection rate, survival rate, and histopathological changes in skin tissue, were evaluated. Overall, our study aims to elucidate the effects and mechanisms of AMPs against AngHV infection and to provide evidence for their development as effective anti-AngHV agents.

Materials and methods

Cell lines

Eel ovary (EO) cells were maintained at the Institute of Biotechnology, Fujian Academy of Agricultural Sciences (FAAS), Fuzhou, China. EO cells were cultured in Leibovitz's L-15 medium (HyClone, USA) supplemented with 10% fetal bovine serum (FBS, Gibco, USA) at 25°C. HEK 293T cell line was purchased from the National Collection of Authenticated Cell Cultures (Shanghai, China) and cultured in DMEM (HyClone) supplemented with 10% FBS (Gibco) at 37°C, 5% CO_2 incubator.

Viruses

AngHV (strain NA16108) was isolated and maintained at the Institute of Biotechnology, Fujian Academy of Agricultural Sciences, Fuzhou, China. AngHV was propagated in EO cells, and then the culture medium was collected until cytopathic effects (CPE) were observed. After the removal of cell debris by centrifugation, the viral titer (half of the tissue culture infectious dose, $TCID_{50}$) was determined by the Reed-Muench method [30].

Peptide chemical synthesis

Peptides, including LJ-hep2 (accession number AY604195) and its derivant peptides (LJ-hep2$_{66–74}$, LJ-hep2$_{72–81}$, and LJ-hep2$_{A4A5}$), AA-hep (accession number XM_035410112.1), Scyampcin$_{44–63}$ (accession number MW388710), Moronecidin$_{23–44}$ (accession number MK387855), OM-hep$_{41–49}$ (accession number AF281354), AS-hep3$_{74–82}$ (accession number AY669378), LC-hep$_{64–72}$ (accession number EU443735.1), PM-hep3$_{67–75}$ (accession number AY574220), LJ-hep2-biotin and AA-hep-biotin, were chemically synthesized by Nanjing GenScript Biotech Co., Ltd. (China), purified by RP-HPLC, and confirmed by MALDI-TOF MS. The purity of the synthetic peptide was higher than 95%. The peptide powder was dissolved in ultrapure water to make the stock solution, which was stored at −20°C.

Cell viability assay

EO cells were seeded into 96-well plates and cultured overnight. Cells were treated with different

concentrations of LJ-hep2, AA-hep, Scyampcin$_{44–63}$, Moronecidin$_{23–44}$, LJ-hep2$_{66–74}$, LJ-hep2$_{72–81}$, LJ-hep2$_{A4A5}$, OM-hep$_{41–49}$, AS-hep3$_{74–82}$, LC-hep$_{64–72}$, and PM-hep3$_{67–75}$ (1, 6.25, 12.5, 25, and 50 μM) at 27°C, respectively. After 48 h, the cytotoxicity of the peptides was determined using the CellTiter 96® AQueous Non-Radioactive Cell Proliferation Assay (Promega, USA) according to the manufacturer's instructions.

AMP screening assay

EO cells were treated with both AngHV (0.1 MOI) and peptides (LJ-hep2, AA-hep, Scyampcin$_{44–63}$, and Moronecidin$_{23–44}$) at the indicated concentrations (1, 6.25, 12.5, 25, and 50 μM) for 1 h simultaneously. Following established protocols for herpesvirus replication assays [31], supernatant samples were collected at 48 h post-infection (hpi), corresponding to the completion of one full viral replication cycle, to ensure measurement of primary virus production prior to substantial secondary infection. After collection, viral DNA copy numbers were quantified by quantitative real-time PCR (qPCR), and the half inhibitory concentration (IC_{50}) of AMPs was subsequently calculated.

Determination of the viral load by qPCR

In 12-well plates, EO cells were treated with both AngHV (0.1 MOI) and LJ-hep2/AA-hep (12.5 μM). After 1 h of incubation, washed three times with PBS, and fresh culture medium was added to the cells. At 48 hpi, AngHV genome copies were detected by qPCR. In the viral growth curve assay, EO cells underwent the same treatment as described above. Subsequently, cells were collected at 6, 12, 24, and 48 hpi, and intracellular viral copies were detected using qPCR.

Genomic DNA was extracted using the TIANamp Marine Animals DNA Kit (TIANGEN, China) following the manufacturer's instructions. Viral load was quantified by qPCR [32]. The recombinant plasmid was serially diluted, and then the AngHV copy number standard curve was prepared using the QuantStudio 3 Real-Time PCR System (Applied Biosystems, USA). TB Green® Premix Ex Taq™ II (TaKaRa) was used to perform the qPCR. The qPCR was performed under the following cycling conditions: 95°C for 30 s, followed by 40 cycles of 95°C for 5 s and 60°C for 34 s. Used Primers were listed in the S1 Table.

Western blotting

EO cells were treated with both AngHV (0.1 MOI) and LJ-hep2/AA-hep (12.5 μM) and performed the same operation as above. At 48 hpi, the abundance of capsid protein, AngHV-ORF36, intracellular was detected by western blotting.

Samples were loaded to SurePAGE™ precast gel and transferred to the polyvinylidene difluoride (PVDF) membrane. The membranes were blocked by 5% skimmed milk for 2 h and incubated with primary antibodies overnight. The primary antibodies were anti-AngHV-ORF36 (Rabbit polyclonal antibody, 1:1000) [33] and anti-α-tubulin (Rabbit polyclonal antibody, 1:5000; Proteintech Group, USA). Next, IRDye® 680RD Goat anti-Rabbit IgG (1:5000; Li-Cor, USA) was used as a secondary antibody to detect the binding at room temperature for 1 h. Imaging was performed using the Odyssey Infrared Imaging System (Li-Cor), and the data were analyzed by ImageJ software.

Cytopathic effects (CPE) assay

CPE assay was used to detect the ability of peptides to inhibit AngHV infection of EO cells. Briefly, cells were infected with AngHV (0.1 MOI) in the presence or absence of LJ-hep2/AA-hep (12.5 μM). Incubation was continued at 27°C until obvious cytopathic effects were observed in the control group (PBS), and the virus titers were determined by use of $TCID_{50}$ assay.

Time-of-addition assay

The Antiviral effect of the LJ-hep2 was determined by using three processing methods. (i) Virus pre-treatment : AngHV (0.1 MOI) was preincubated with LJ-hep2 (6.25 and 12.5 μM) or PBS at 27°C for 1 h. The mixture was then added to EO cells for 1 h. Afterward, the cells were washed three times with PBS, and the fresh complete culture medium was added to the cells; (ii) Cell pre-treatment: EO cells were incubated with LJ-hep2 (6.25 and 12.5 μM) or PBS for 1 h (27°C). Subsequently, cells were washed thrice with PBS and infected with AngHV (0.1 MOI) for 1 h. Then, the cells were washed three times with PBS, and the fresh culture medium was added; (iii) Post-treatment: EO cells were infected by AngHV (0.1 MOI) for 1 h at 27°C. Then, the cells were washed thrice with PBS, treated with LJ-hep2 (6.25 and 12.5 μM) or PBS for 1 h, washed with PBS, and fresh culture medium was added. After 48 hpi, EO cells and culture supernatants from each group were collected separately. Genomic DNA was extracted from the harvested cells, and AngHV copy numbers were quantified by qPCR. The collected supernatants were inoculated onto freshly prepared EO cells to observe CPE, and virus titers ($TCID_{50}$) were calculated using the Reed-Muench method.

Viral binding assay and internalization assay

EO cells were infected with AngHV (0.1 MOI) and treated with 12.5 μM LJ-hep2 for 1 h at 4°C. Cells were then washed with pre-cooled PBS. After washing to remove the unbound viruses, cells were lysed, and viral DNA copies were determined by qPCR.

EO cells were infected with AngHV (0.1 MOI) for 1 h at 4°C to allow the virus to attach to the cell surface. Then, 12.5 μM LJ-hep2 was added to the cells after washing with pre-cooled PBS, and the cells were incubated at 27°C. After 1 h of treatment, LJ-hep2 was removed, and the cells were sequentially washed with PBS containing 0.05% trypsin and with PBS alone. qPCR was used to detect the amount of virus internalization.

Fluorescence analysis and flow cytometry

AngHV (0.1 MOI) was subjected to treatment with PBS or 12.5 μM LJ-hep2/AA-hep for 1 h at 27°C. Subsequently, the mixture was added to EO cells and maintained at 27°C. At 1 hpi, the inoculum was removed, and the cells underwent three washes. Following this, the cells were fixed with 4% paraformaldehyde, permeabilized with 0.1% Triton X-100, and stained with anti-AngHV-ORF36 (Rabbit polyclonal antibody, 1:500) [33] and Alexa Fluor 488-Labeled Goat Anti-Rabbit IgG (Beyotime, China) at a dilution of 1:500. Nuclei were stained in blue with DAPI (Sigma-Aldrich, USA), and filamentous actin was stained in red with Alexa Fluor 555 labeled phalloidin (Invitrogen, USA). Fluorescence microscopy using a BZ-X800LE (Keyence, Japan) was employed for cell detection, and ImageJ software was utilized for data analysis. Flow cytometry was performed using an Accuri^{TM} C6 (BD Biosciences, USA), and the data were analyzed by FlowJo software (Tree Star, USA).

Assessment of gene expression by qPCR

Total RNA was extracted from EO cells using TRIzol reagent (Invitrogen) according to the manufacturer's instructions. RNA (500 ng) was reverse-transcribed using the PrimeScript^{TM} RT Reagent Kit with gDNA Eraser (TaKaRa, Japan) according to the manufacturer's instructions. Genomic DNA and cDNA samples were stored at −80°C until use.

The expression patterns of different genes (including IFNα, TNFα, MxC, and IL-8; accession numbers XM035397141.1, MT861110.1, KC430926.1, and MT861113.1) were examined by qPCR, and RPL7 (accession number MK929311) was used as the housekeeping gene [34]. The PCR cycling conditions were consistent with those described above. The dissociation curves for each gene were plotted to demonstrate the specificity of the primers. The relative expression levels were calculated using the $2^{-\Delta\Delta Ct}$ method based on the threshold cycle (Ct) values [35]. Primers of genes were designed using Primer 5.0 software and were listed in the S1 Table.

Inactivation of cell-free virions

The ability of LJ-hep2/AA-hep to inactivate cell-free virions was measured. Briefly, LJ-hep2/AA-hep was mixed with an equal volume of AngHV (0.1 MOI) [36]. After incubation for 1 h at 27°C, a final concentration of 3% PEG-6000 (Leagene, China) was added to the mixture and incubated for another 1 h at 4°C. After centrifugation at 13,000 rpm, 4°C for 30 min, the supernatant was discarded, and the pellet was washed twice with 3% PEG-6000 (Leagene) containing 10 mg/mL BSA. Finally, the pellet was re-suspended in the medium and added to the EO cells. After incubation at 27°C for 48 h, the viral load in the cells was measured by qPCR.

Transmission electron microscopy (TEM) assay

To determine the effect of LJ-hep2 and AA-hep on viral particles, virions were isolated and purified [37]. AngHV (10^6 copies) was treated with PBS, LJ-hep2 (0.05 mg/mL), and AA-hep (0.05 mg/mL) for 1 h. Subsequently, the sample was pipetted onto pure formvar support films for 5 min. Afterward, the films were edge-blotted with filter paper to remove the excess sample, then transferred to 1% phosphotungstic acid and incubated for 1 min. After removal of the solution, the films were air-dried at room temperature and then imaged using Hitachi HT7700 TEM (Hitachi, Japan).

MNase digestion assay

Purified AngHV virions (10^7 copies) were incubated with PBS, LJ-hep2, AA-hep, LJ-hep2$_{66-74}$, LJ-hep2$_{72-81}$, LJ-hep2$_{A4A5}$, OM-hep$_{41-49}$, AS-hep3$_{74-82}$, LC-hep$_{64-72}$, and PM-hep3$_{67-75}$ (12.5 μM) at 27°C for 1 h. Then, the mixture was digested with micrococcal nuclease (New England BioLabs, USA) at 37°C for 1 h [38]. Afterward, the undigested viral genomic DNA was extracted and quantified by qPCR.

Peptide-virus binding assay

LJ-hep2/AA-hep (0.2, 1, and 5 μg per well) were coated onto 96-well ELISA plates and incubated at room temperature for 1 h. The plates were then blocked with 2%

BSA at 4°C overnight. Purified AngHV virions (10^6 copies per well) were added to the ELISA plates and incubated at room temperature for 1 h. After washing, the bound viruses were lysed with the GA buffer of TIANamp Genomic DNA Kit (TIANGEN) for viral DNA extraction, and then measured by qPCR.

AngHV (10^4, 10^5, and 10^6 copies per well) were coated onto 96-well ELISA plates and incubated at 4°C for 8 h. Then, 2% BSA was used to block plates at 4°C overnight. LJ-hep2/AA-hep (5 μg per well) were added for binding to the coated viruses at room temperature for 1 h. After washing, the bound peptide was detected by Rabbit anti-biotin (Proteintech Group) with secondary Goat-anti-Rabbit HRP (Abcam) by reading OD_{450}.

Peptide-protein docking

The 3D structure modes of AngHV-ORF51, LJ-hep2/AA-hep, and the structure of protein-peptide complexes were obtained by using the HPEPDOCK program [39]. PyMOL software was used to visualize and analyze these structure models [40]. The best complex with the highest score was chosen for the following docking analysis.

Pull-down analysis

To achieve transient expression of ORF51, the pcDNA3.1-ORF51-HA plasmid was constructed. HEK 293T cells were seeded overnight and transfected with pcDNA3.1-ORF51-HA by using Lipofectamine™ 3000 Transfection Reagent (Invitrogen). At 24 h post-transfection, the cells were harvested and lysed in RIPA lysis buffer (Beyotime). The clarified supernatants were incubated with 12.5 μM biotin-labeled LJ-hep2 and AA-hep for 4 h at 4°C, and then incubated with 20 μL BeyoMag™ Streptavidin Magnetic Beads (Beyotime) overnight at 4°C. After three times washing with PBS, beads were boiled in 1×loading buffer for 10 min to elute protein complexes.

Subsequently, the samples were subjected to the immunoblotting assay. Anti-HA (Mouse monoclonal antibody, 1:1000; Servicebio, China) and IRDye® 800RD goat-anti Mouse IgG (1:5000; Li-Cor) were used as primary and secondary antibodies, respectively. Imaging was performed using the Odyssey Infrared Imaging System (Li-Cor), and the data were analyzed by ImageJ software.

Stability assay of LJ-hep2

Aquaculture water (AW) was obtained from the water flow system. LJ-hep2 (12.5 μM) was dissolved in sterilized AW samples at 27°C for multiple time points (6 h, 12 h, and 24 h), up to 24 h (12/12 h dark/light). LJ-hep2 dissolved in ultrapure water was used as a control. Then, EO cells were treated with LJ-hep2 (samples from multiple time points) and AngHV (0.1 MOI) simultaneously. At 48 hpi, cells were collected, and total DNA was extracted for viral copy number detection by qPCR.

Animal experiments

American eels (*A. rostrata*) were obtained from the Institute of Biotechnology, Fujian Academy of Agricultural Sciences (FAAS), Fuzhou, China. Captured glass eels (*A. rostrata*) were cultured in a flow system containing aerated water and fed twice daily at 2% of their total biomass. After three months, eels were selected based on body weight (3.5 g ±0.3 g), and 5% were used for pre-testing to confirm the absence of AngHV infection [9]. Then, *A. rostrata* were randomly grouped (10 eels per group) for the acute toxicity assay by exposing them to a range of LJ-hep2 (0.25, 0.5, and 1 mg/L). Mortality was recorded daily for 5 days.

Median/absolute infectious dose ($ID_{50/100}$): Eels (*A. rostrata*; $n = 15$) were infected with AngHV (10^0-10^5 $TCID_{50}$/mL) by immersion bath [41]. After 6 h, the container water was renewed totally, and infected fish were reared for an additional 3 days. Subsequently, all eels were anesthetized with tricaine methanesulfonate (MS-222; Sigma-Aldrich), and then visceral tissues (including liver, spleen, and kidney) were collected from each fish and tested for viral content by qPCR. A linear regression curve was drawn according to the infection rate and infection dose, and $ID_{50/100}$ was calculated.

Eels (*A. rostrata*) were randomly divided into two groups (21 eels per group). The eels were infected with ID_{50} of AngHV ($10^{1.5}$ $TCID_{50}$/mL) in the presence or absence of LJ-hep2 (1 mg/L). After a 6-hour exposure period, the culture water of each group was completely renewed. At 72 hpi, visceral tissues of eels (including liver, spleen, and kidney) were sampled to detect viral copies and infection rates.

Horizontal transmission assay

American eels were randomly divided into three groups. One group was left untreated as a mock group (10 eels). On the other hand, 10 donor eels were exposed to ID_{100} of AngHV (10^4 $TCID_{50}$/mL) for 24 h. Then, 5 donor fish were randomly mixed into the peptide treatment group (25 recipient eels)/AngHV group (25 recipient eels) in the presence or

absence of LJ-hep2 (0.5 mg/L). The aquatic water (with or without 0.5 mg/L LJ-hep2) of each group was completely renewed daily for an additional 2 days. After 3 days of mixed breeding, the number of recipient fish (n = 10) infected with AngHV was determined by qPCR. The mortality was recorded daily for 21 days (n = 20). At 21 dpi, skin tissue slices of eels were taken from each group and then stained with hematoxylin and eosin (H&E) according to the previous study [42,43].

Statistical analysis

Statistically analyzed data were presented as the mean ± standard deviation (SD). Biological replicates are indicated in figure legends. The blotting band and fluorescence signal intensities were determined using the ImageJ software (NIH, USA). For intergroup comparisons, statistical significances were analyzed with an unpaired two-tailed Student's t-test, two-way analysis of variance (ANOVA), and Log-rank (Mantel-Cox) Test (for survival data only) using Prism 8 software (GraphPad, USA). $p < 0.05$ was considered to indicate statistical significance.

Results

Anti-AngHV activity of marine antimicrobial peptides

Previous studies have reported that marine-derived peptides can influence the infection of several viruses [44]. To explore the anti-AngHV infection activity of marine AMPs, we first obtained a hepcidin gene of the European eel *A. anguilla* (AA-hepcidin). The open reading frame (ORF) sequence of this gene was verified by PCR to be 270 bp in length, encoding 89 amino acids (S1 Fig). Notably, the amino acid sequence of 69th to 89th of AA-hepcidin showed a high sequence identity with the amino acid sequence of 66th to 86th of LJ-hepcidin2 (LJ-hep2, derived from Japanese seabass *L. japonicus*). We further chemically synthesized AA-hepcidin$_{69-89}$ (AA-hep) for subsequent antiviral screening together with three AMPs previously reported by our laboratory (LJ-hep2, Scyampcin$_{44-63}$, and Moronecidin$_{23-44}$).

Antiviral peptide screening was performed in EO cells, which are highly susceptible to AngHV infection. EO cells were exposed to the four selected AMPs, and the cytotoxicity of AMPs was assessed. Meanwhile, EO cells were infected with AngHV in the presence of different AMPs, and viral DNA in the cell supernatant was quantified by qPCR at 48 hpi. The results demonstrated that LJ-hep2 and AA-hep significantly inhibited AngHV reproduction in EO cells, whereas Scyampcin$_{44-63}$ and Moronecidin$_{23-44}$ had weak antiviral activity (Figure 1(A–D), Table 1). Both LJ-hep2 and AA-hep showed no obvious cytotoxicity, and their 50% cytotoxicity concentration (CC_{50}) could not be calculated (Table 1). The 50% inhibitory concentration (IC_{50}) for AngHV was determined to be 5.8 μM and 10.3 μM for LJ-hep2 and AA-hep, respectively (Table 1). The calculated selectivity index (SI, CC_{50} /IC_{50}) for LJ-hep2 and AA-hep was greater than 8.6 and 4.9, respectively, indicating that they had substantial anti-AngHV potential (Table 1). These results prompted us to further investigate the anti-AngHV effects of LJ-hep2 and AA-hep.

Comparative analysis of antiviral activity in vitro between LJ-hep2 and AA-hep

According to the above results, we found that the antiviral activity of AA-hep was relatively weak. Therefore, a concentration of 12.5 μM was selected for follow-up studies to ensure viral inhibition rates of both peptides exceeded 50%. EO cells were infected with AngHV in the presence of peptides for 1 h, washed three times, and then cultured with fresh medium (Figure 1(E)). At 48 hpi, compared to the control (PBS), both LJ-hep2 and AA-hep significantly reduced the abundance of the viral capsid protein ORF36 and suppressed the replication of the viral genome (Figure 1(F,G)). The results of the viral growth curve assay showed that LJ-hep2 and AA-hep remarkably inhibited viral reproduction in a time-dependent manner (Figure 1(H)). Next, we examined the effects of LJ-hep2 and AA-hep on viral titers and virus-induced cytopathic effects (CPE). As shown in Figure 1(I), AngHV titers were significantly decreased regardless of the presence of either peptide. Additionally, LJ-hep2 and AA-hep effectively alleviated AngHV-induced CPE (Figure 1(J)). These findings collectively demonstrated the inhibitory effects of LJ-hep2 and AA-hep on intracellular viral genome replication and extracellular viral titers. Notably, LJ-hep2 exhibited a stronger anti-AngHV effect than AA-hep. Therefore, we proceeded to further characterize the anti-AngHV properties of LJ-hep2.

LJ-hep2 inhibits AngHV infection by affecting viral binding

To explore how LJ-hep2 affects viral infection, we first examined the effects of LJ-hep2 on innate immune responses. Viral infections can stimulate intrinsic cellular immune defense responses, including activation of cytokine pathways, leading to the secretion of cytokines

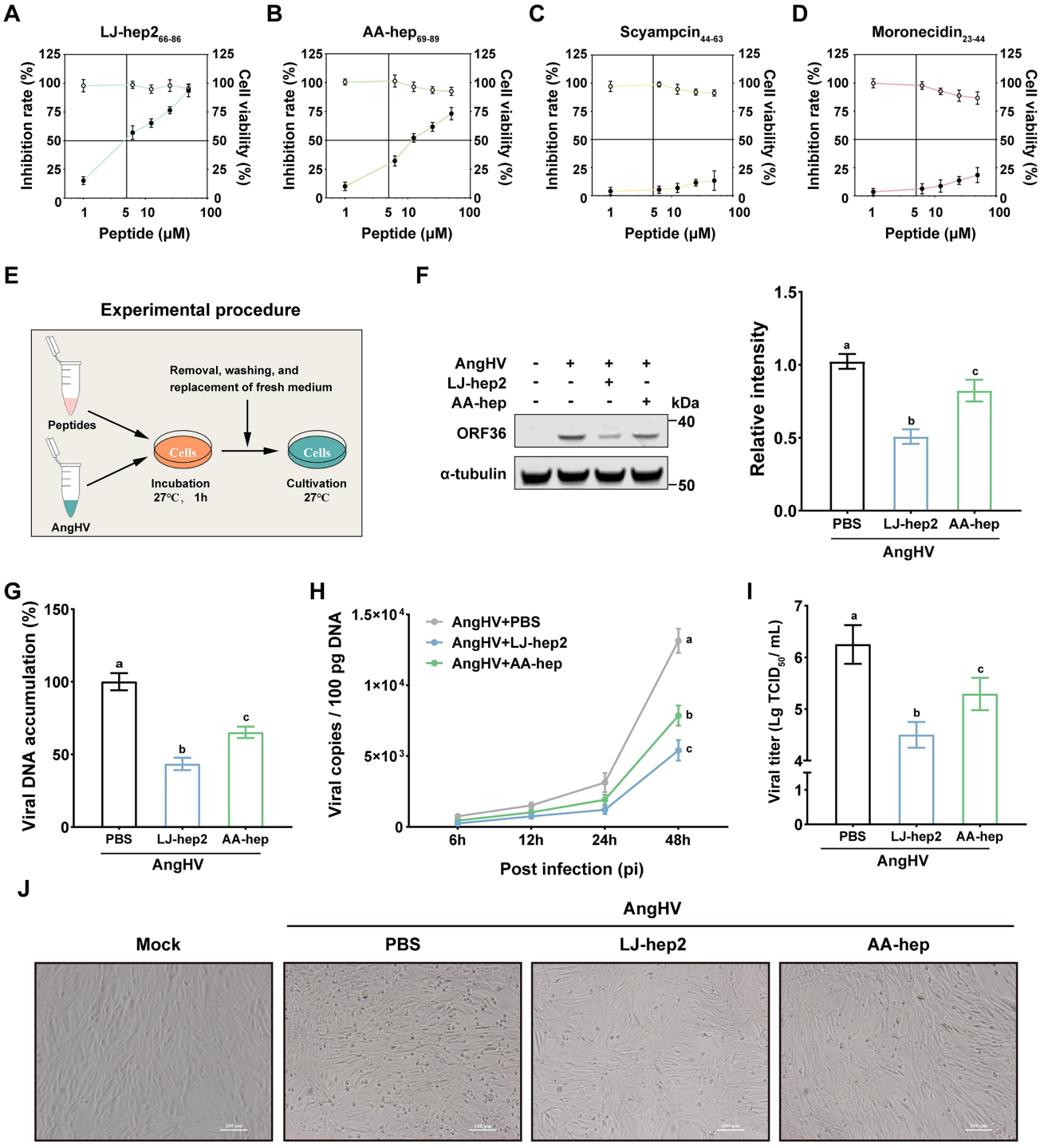

Figure 1. Anti-AngHV activity of the marine antimicrobial peptides (A-D) MTS analysis assessed EO cell viability following peptide treatments, while qPCR quantified viral copy numbers in cells treated with peptides and AngHV. The inhibition rate is shown as solid points; Cell viability is shown as empty points. Peptides tested were LJ-hep2 (A), AA-hep (B), Scyampcin$_{44-63}$ (C), and Moronecidin$_{23-44}$ (D). (E) Schematic of virus infection assay workflow. (F) EO cells were simultaneously treated with LJ-hep2/AA-hep (12.5μM) and AngHV (0.1 MOI). At 48 hpi, viral capsid protein (ORF36) in the infected cells was quantified by western blotting, using α-tubulin as a loading control. (G) EO cells were simultaneously treated with LJ-hep2/AA-hep (12.5μM) and AngHV (0.1 MOI) for 1h. At 48 hpi, the viral DNA level in the cell lysate was measured by qPCR. (H) The growth curve of AngHV in the PBS and LJ-hep2 /AA-hep (12.5μM). Viral DNA level was measured by qPCR at multiple time points post-infection (6, 12, 24, and 48 hpi). (I) EO cells were simultaneously treated with LJ-hep2/AA-hep (12.5μM) and AngHV (0.1 MOI). Viral titer was determined by TCID$_{50}$ assays. TCID$_{50}$, 50% tissue culture infective dose. (J) EO cells infected with AngHV (0.1 MOI) in the presence or absence of LJ-hep2/AA-hep (12.5μM), and CPE of EO cells were observed by microscopy at 5 dpi (scale bar=100μm).

The data were representative of three independent replicates and expressed as mean ± SD ($n = 3$). Differences in different groups were indicated with the letter "a," "b" or "c".

Table 1. Some properties of the selected marine peptides.

Peptides	Species	Sequences	N	NC	H	pI	MW	CC_{50}	IC_{50}	SI
LJ-hep2	*Lateolabrax maculatus*	IKCKFCCGCCTPGVCGVCCRF	21	+3	86.3%	8.53	2231	>50	5.8	>8.6
AA-hep	*Anguilla anguilla*	SLCRYCCNCCKNKGCGYCCRF	21	+4	59.5%	8.73	2428	>50	10.3	>4.9
$Scyampcin_{44–63}$	*Scylla paramamosain*	GKKKKRNMMKTKEPGIIFFF	20	+6	21.1%	10.68	2429	>50	>50	ND
$Moronecidin_{23–44}$	*Sebastiscus marmoratus*	FFRHIVGAISRIFGQKQRDMAD	22	+2	36.0%	10.74	2593	>50	>50	ND

N, the number of amino acids. NC, the net charge of AMPs at neutral pH. H, the hydrophobicity of AMPs. pI, the isoelectric point of AMPs. MW, the molecular weight (Da) of AMPs. CC50, the 50% cytotoxic concentration of peptides to EO cells. IC50, the 50% inhibitory concentration of peptides against AngHV. SI, the value of CC50/IC50. "ND" represents measurements that were not determined.

such as type I interferon (IFN-I), tumor necrosis factor (TNF-α), and interleukins, as well as the production of antiviral proteins like myxovirus resistance protein C (MxC) [45]. Therefore, to determine whether the antiviral effects of LJ-hep2 were attributed to its induction of the IFN-I and/or cytokine antiviral pathways, we assessed the effects of LJ-hep2 treatment on the expression levels of several cytokine-related genes. The results showed that LJ-hep2 treatment did not affect the expression of IFN-α, TNF-α, interleukin-8 (IL-8), and an antiviral protein MxC in the presence or absence of AngHV infection (S2A Fig). In contrast, AngHV infection markedly upregulated the expression of IFN-α, MxC, TNF-α, and IL-8, and this virus-induced upregulation was significantly suppressed when LJ-hep2 was administered concurrently with viruses (S2B Fig). It indicated that LJ-hep2 might not inhibit AngHV infection by inducing antiviral cytokine production.

The viral life cycle typically involves three major stages: (1) early stage (binding/internalization), (2) intermediate stage (translation/replication), and (3) late stage (assembly/release). To determine which stage of AngHV infection was affected by LJ-hep2, a time-of-addition assay was conducted in EO cells. The schematic diagrams of each treatment were detailed in Figures 2(A,D,G). We found that LJ-hep2 significantly reduced intracellular viral DNA accumulation and extracellular progeny virus production in a dose-dependent manner in the virus pre-treatment group (Figure 2(B,C)), whereas LJ-hep2 had no effect on AngHV infection in the cell pre-treatment group (Figure 2(E,F)) and post-treatment group (Figure 2(H,I)). These findings suggested that LJ-hep2 might affect the early stage of AngHV infection. We next assessed the ability of the LJ-hep2 interfering virus to bind or internalize host cells (Figure 2(J)). As shown in Figures 2(K,L), LJ-hep2 significantly affected viral binding and did not affect viral internalization. These data suggested that LJ-hep2 might prevent viral entry into cells by affecting viral binding.

LJ-hep2 inhibits AngHV infection by directly interacting with virions

Viral binding is the first step of viral entry into cells, and interference with this process may directly reduce viral entry. Following an established approach for viral entry assessment [46], fluorescence microscopy for qualitative observation and flow cytometry for quantitative analysis were employed. The viral dose was kept consistent with the antiviral activity experiments to ensure direct comparability of peptide effects under identical conditions. The inhibitory effect of LJ-hep2 on viral entry was assessed in EO cells, with AA-hep included for comparison. The schematic diagram is shown in Figure 3(A). Fluorescence microscopy observations revealed that LJ-hep2 significantly hindered viral entry, with stronger inhibition compared to AA-hep (Figure 3(B,C)). Quantitative analysis of viral entry using flow cytometry showed that LJ-hep2 inhibited AngHV entry into host cells more strongly than AA-hep (Figure 3D), confirming the superior antiviral efficacy of LJ-hep2 in reducing viral infection.

To further rule out the effect of the peptides, an incubation of cell-free virions assay was performed. It was found that the cell-free virions pretreated with LJ-hep2 or AA-hep lose their infectivity (Figure 3(E)). TEM analysis was conducted to delve into the effects of the two peptides on virions, and the results showed that LJ-hep2 induced substantial alterations in AngHV ultrastructure, resulting in loss of viral integrity, whereas the effect of AA-hep was less pronounced (Figure 3(F)). The disruption of the virion allowed externally added micrococcal nuclease to degrade the viral genome. Pre-incubation of AngHV with LJ-hep2 significantly reduced the percentage of genome copy equivalents (GCE) compared to the PBS- and AA-hep-treated groups (Figure 3(G)). These results suggested that the destruction of virions due to peptide-virus interactions might be the main reason for the inhibition of AngHV infection.

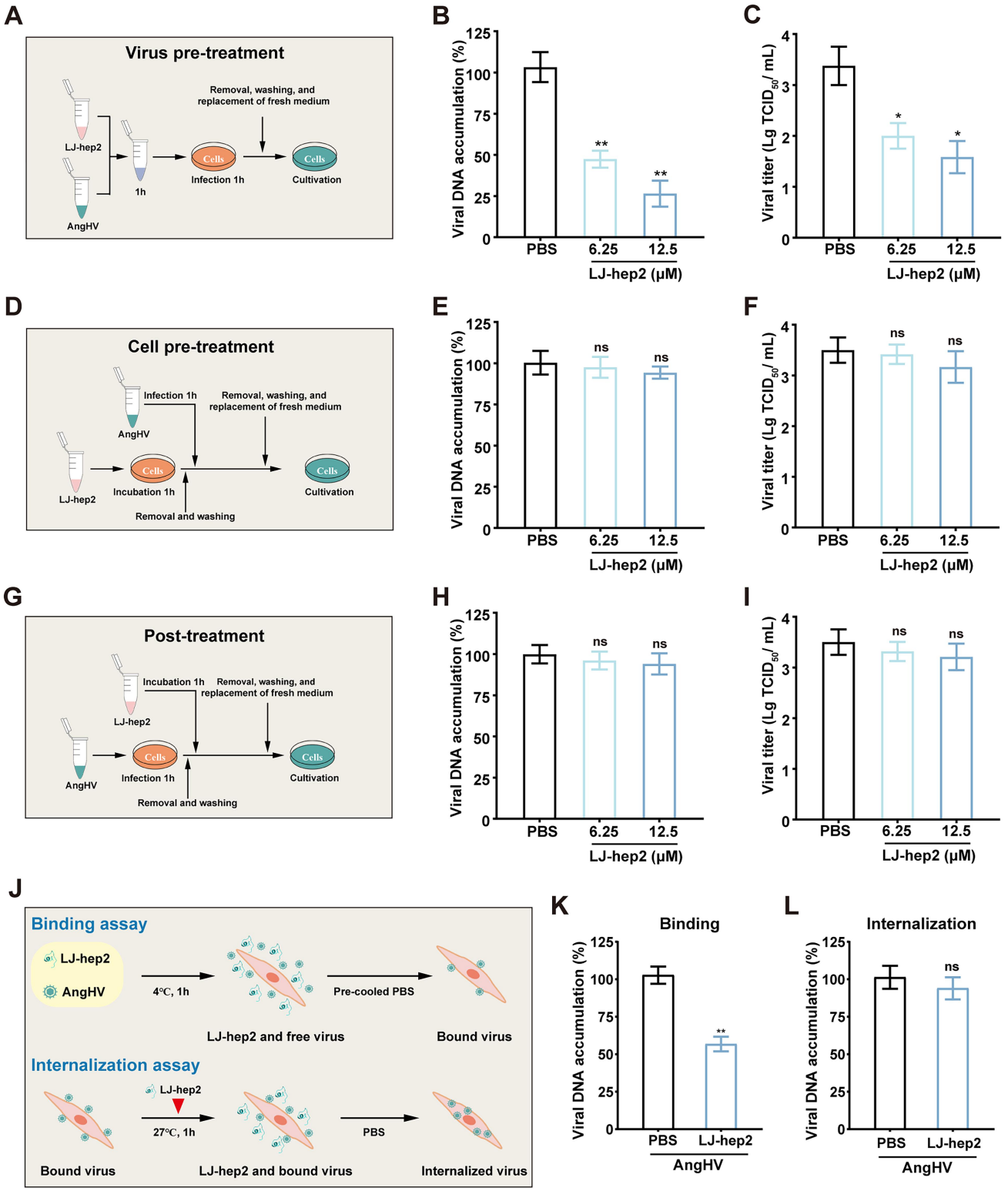

Figure 2. LJ-hep2 inhibits AngHV infection by influencing viral binding (A) Schematic of virus pretreatment assay workflow. (B and C) The intracellular AngHV DNA level (48 hpi) and the viral titer in the virus pre-treatment way. (D) Schematic of cell pre-treatment assay workflow. (E and F) The intracellular AngHV DNA level (48 hpi) and the viral titer in the cell pre-treatment way. (G) Schematic of post-treatment assay workflow. (H and I) The intracellular AngHV DNA level (48 hpi) and the viral titer in the post-treatment way. (J) Schematic workflow of the binding and internalization assays. (K) AngHV (0.1 MOI) and LJ-hep2 (12.5μM) were added to the cells for 1h at 4°C. At 48 hpi, the viral DNA level of the binding assay was measured by qPCR. (L) AngHV (0.1 MOI) was added to the cells for 1h at 4°C, then the virus-bound cells were incubated with LJ-hep2 (12.5μM) for 1h at 27°C. At 48 hpi, the viral DNA level of the internalization assay was measured by qPCR.

The data were representative of three independent experiments and expressed as mean ± SD ($n = 3$). ns: not significant, **: $p < 0.01$.

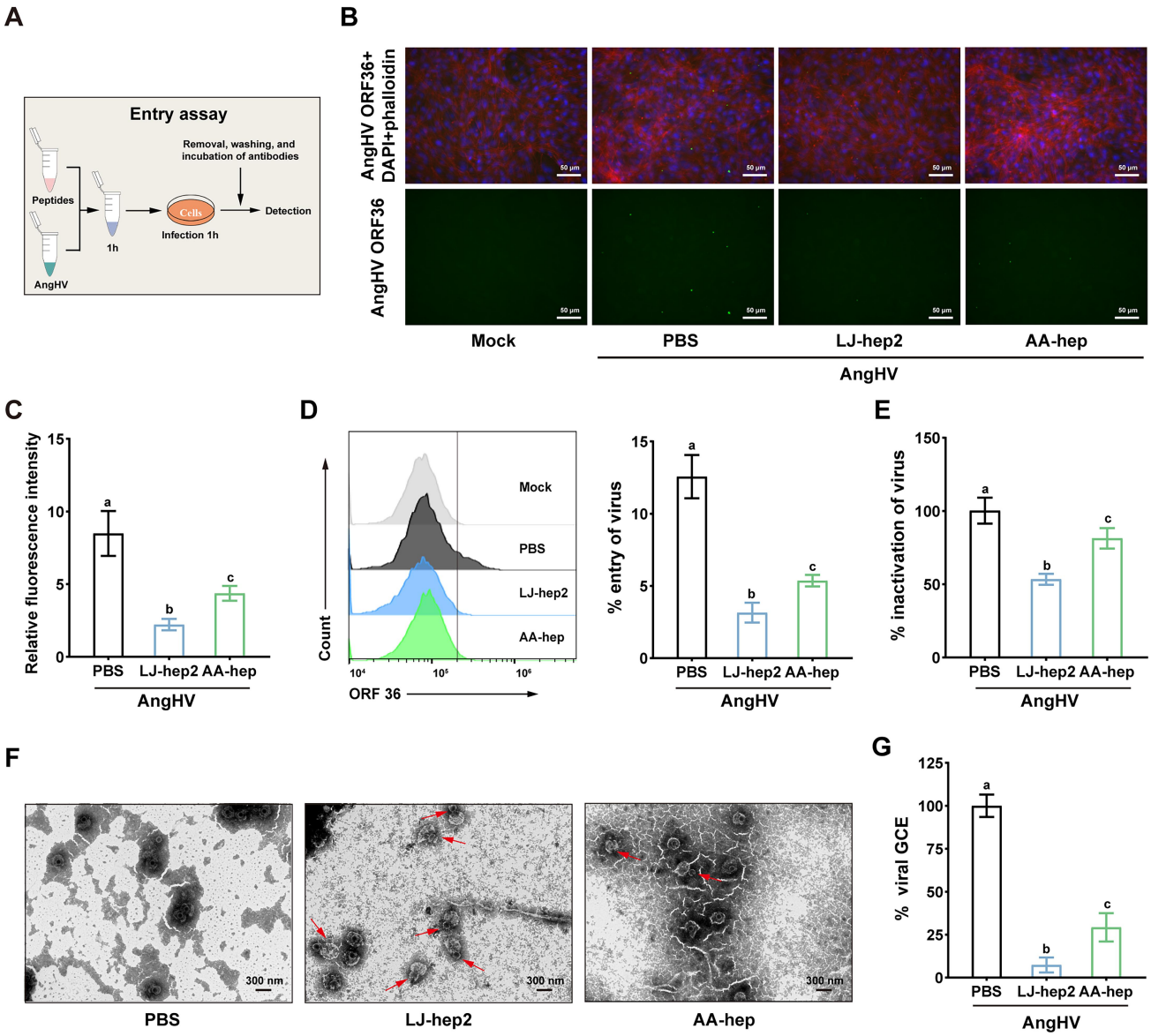

Figure 3. LJ-hep2 inhibits AngHV infection by directly interaction with virions.

(A) Schematic of entry assay workflow. (B) AngHV (0.1 MOI) was pre-incubated with LJ-hep2/AA-hep (12.5 μM) for 1 h, then the mixture infected EO cells at 27°C. At 1 hpi, the cells were detected under a fluorescence microscope (scale bar = 50 μm). (C) The indicated fluorescence signals were quantified using ImageJ software. (D) AngHV (0.1 MOI) was pre-incubated with LJ-hep2/AA-hep (12.5 μM) for 1 h, then the mixture infected EO cells at 27°C. At 1 hpi, flow cytometry was used to measure the amount of virus entering the cells. (E) LJ-hep2 /AA-hep (12.5 μM) was mixed with AngHV (0.1 MOI) and incubated for 1 h. Then PEG-6000 was added to the mixture and the resuspended virus particles infected EO cells. The intracellular AngHV copies were quantified by qPCR. (F) TEM analysis of AngHV (10^6 copies) exposed to LJ-hep2 and AA-hep (0.05 mg/mL, scale bar = 300 nm). The red arrows indicate broken virions. (G) MNase digestion experiment was used to detect the genomic DNA unreleased by AngHV (10^7 copies) treated with LJ-hep2 and AA-hep (12.5 μM). The data were representative of three independent experiments and expressed as mean ± SD ($n = 3$). Differences in different groups were indicated with the letter "a," "b" or "c".

LJ-hep2 inactivates AngHV by binding to the viral envelope protein ORF51

Given the observed possible direct interaction between the peptides and the virions, we conducted a comprehensive evaluation of the binding of LJ-hep2 /AA-hep to AngHV. The results showed that both peptides captured AngHV virions in a dose-dependent manner (Figure 4(A)) and that LJ-hep2-biotin/AA-hep-biotin bound to AngHV virions in a quantity-dependent manner (Figure 4(B)). Importantly, LJ-hep2 had a closer integration with AngHV than AA-hep (Figure 4(A,B)). This difference in binding ability might account for the superior antiviral activity of LJ-hep2 compared with that of AA-hep, prompting

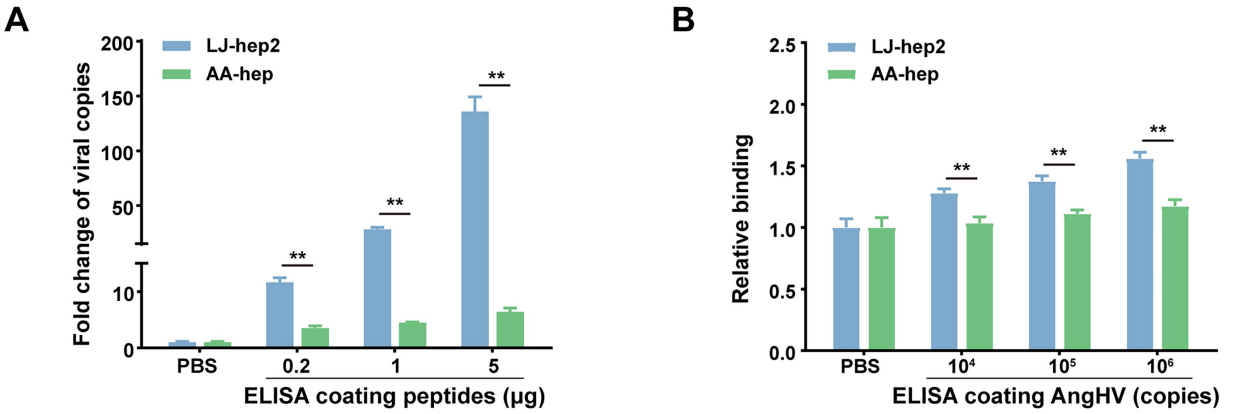

C

Receptor	HPEPDOCK score Ligands	
	LJ-hep2	AA-hep
ORF51	-218.042	-198.617
ORF49	-217.866	-224.005
ORF108	-215.852	-248.207
ORF78	-204.428	-228.341
ORF67	-194.789	-209.243
ORF71	-193.833	-198.672
ORF125	-193.670	-231.836
ORF8	-189.254	-193.419
ORF115	-180.878	-201.421
ORF95	-180.594	-191.701
ORF66	-164.046	-213.553

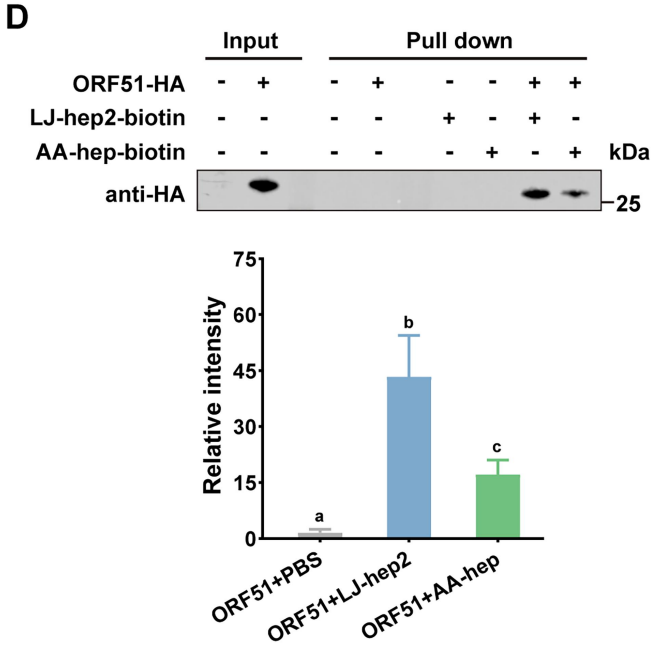

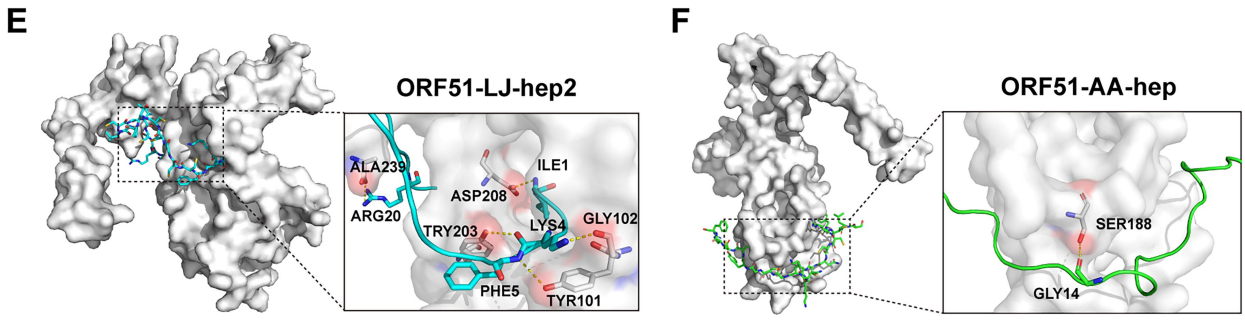

G

Peptides	Sequence	Bound peptide residues	Bound ORF51 residues	Hydrophobicity
LJ-hep2$_{66–86}$	IKCKFCCGCCTPGVCGVCCRF	ILE-1 LYS-4 PHE-5 ARG-20	ASP-208 TYR-203, GLY-102 TYR-101 ALA-239	0.863
AA-hep$_{69-89}$	SLCRYCCNCCKNKGCGYCCRF	GLY-14	SER-188	0.595

Figure 4. LJ-hep2 inactivate AngHV by binding to the viral envelope protein ORF51.

a comparative analysis of the antiviral mechanisms of the two peptides.

Direct interaction of antiviral factors with viral proteins has long been considered a prevalent antiviral mechanism, especially for enveloped viruses [47]. An earlier study on the identification and localization of the structural proteins of AngHV identified 11 envelope proteins, specifically ORF8, ORF49, ORF51, ORF66, ORF67, ORF71, ORF78, ORF95, ORF108, ORF115, and ORF125 [37]. Using an *in-silico* method, we investigated the interactions of LJ-hep2 and AA-hep with these envelope proteins and summarized their respective binding strengths in Figure 4(C). LJ-hep2 exhibited the strongest binding ability to the viral envelope protein ORF51, with a maximum HPEPDOCK score of −218.042, suggesting that ORF51 May be the main target of LJ-hep2 binding to AngHV (Figure 4(C)). Interestingly, compared with AA-hep, LJ-hep2 exhibited stronger binding ability to ORF51, while weaker binding to all other membrane proteins (Figure 4(C)). The results of the pull-down assay further confirmed the strong interaction between LJ-hep2 and ORF51, underscoring its stronger binding efficiency than AA-hep (Figure 4(D)).

To graphically depict the binding of the peptides to viral envelope protein ORF51, 3D structures of ORF51, LJ-hep2, and AA-hep were generated, as shown in S3A – S3C Fig. Analysis of peptide-protein interactions in the docked complex revealed that LJ-hep2 strongly binds to ORF51 by interacting with five amino acids (ASP-208, TYR-203, GLY-102, TYR-101, and ALA-239; Figure 4(E,G)). In contrast, AA-hep showed weaker binding efficiency, interacting with only 1 amino acid (SER-188; Figure 4F and 4G). This strong binding efficiency to ORF51 May be the key factor behind LJ-hep2's potent antiviral activity.

Detection of key sites where LJ-hep2 exerts antiviral activity

By comparing these two peptide sequences (Figure 5(A)), we found that their amino acid sequences shared a 52.4% identity, with the seven amino acids at the C-terminus being highly conserved. However, their N-terminus amino acid compositions differed considerably, except for the five cysteines, which were conserved. We hypothesized that this non-conserved N-terminal region might be responsible for the differences in their antiviral activities. To test this hypothesis, we truncated LJ-hep2 into two peptides: one containing 9 amino acids at the N-terminus (LJ-hep2$_{66-74}$) and the other containing 10 amino acids at the C-terminus (LJ-hep2$_{72-81}$). Cytotoxicity tests were performed to determine the concentration of these two truncated peptides used to exclude the effect of the peptides on the cells themselves (Figure 5(B)). Furthermore, we observed that LJ-hep2$_{66-74}$ exhibited similar antiviral activity to intact LJ-hep2, including significant inhibition of viral replication, progeny virion production, and disruption of the viral structure leading to leakage of the viral genome (Figure 5(C–E)). These results suggest that the strong anti-AngHV activity of LJ-hep2 is mainly attributed to the N-terminal segment (LJ-hep2$_{66-74}$).

Hepcidin is a conserved AMP identified in various fish species. To understand why the N-terminal segment of LJ-hep2 (LJ-hep2$_{66-74}$) exhibits strong antiviral activity, we compared the amino acid sequences of hepcidin from different fish species. The analysis revealed that the sequence of LJ-hep2$_{66-74}$ differs from that of other fish hepcidins at the Lys-4 and Phe-5 positions (Figure 5(F)). Furthermore, ORF51 transmembrane prediction analysis indicated that these two amino acids of LJ-hep2$_{66-74}$ bind to the transmembrane region of ORF51 (S4 Fig and Figure 4(G)), potentially resulting in conformational changes that would allow LJ-hep2 to effectively disrupt the viral envelope structure. To assess the contribution of Lys-4 and Phe-5 to anti-AngHV activity, we performed an alanine (Ala) substitution experiment, mutated Lys-4 and Phe-5 to Ala, and synthesized the mutant peptide LJ-hep2$_{A4A5}$ (Figure 5(F)). After cytotoxicity testing, we selected a concentration with no apparent cytotoxicity to compare their anti-AngHV activity (Figure 5(F)). The results showed that AS-hep3$_{74-82}$ and LC-hep$_{64-72}$, which share greater sequence similarity to LJ-hep2$_{66-74}$, also exhibited certain antiviral activity,

(A) LJ-hep2/AA-hep (0.2, 1, and 5 μg) and PBS were coated on an ELISA plate. The AngHV virions were added to the ELISA plate for binding. Viral DNA copies were measured by qPCR to show the bound virus. (B) AngHV (10^4, 10^5, and 10^6 copies) and PBS were coated on an ELISA plate. LJ-hep2/AA-hep were added to the ELISA plate for binding. LJ-hep2/AA-hep was detected by rabbit anti-biotin to show the bound LJ-hep2/AA-hep. (C) Docking score of LJ-hep2 and AA-hep with envelope proteins of AngHV. (D) Immunoblotting analysis of AngHV-ORF51 interaction with LJ-hep2 (12.5 μM) and AA-hep (12.5 μM). (E and F) Lowest-energy structure of the complex. The white surface represents ORF51, the blue ribbon represents LJ-hep2, and the green ribbon represents AA-hep. Relative positions of amino acids involved in interactions between ORF51 and LJ-hep2/AA-hep. Yellow dashed lines indicate hydrogen bonds. Sticks indicate directly interacting amino acids. (G) Hydrophobicity of LJ-hep2/AA-hep and potential binding sites between LJ-hep2/AA-hep and ORF51. The data were representative of three independent experiments and expressed as mean ± SD ($n = 3$). Differences in different groups were indicated with the letter "a," "b" or "c." **: $p < 0.01$.

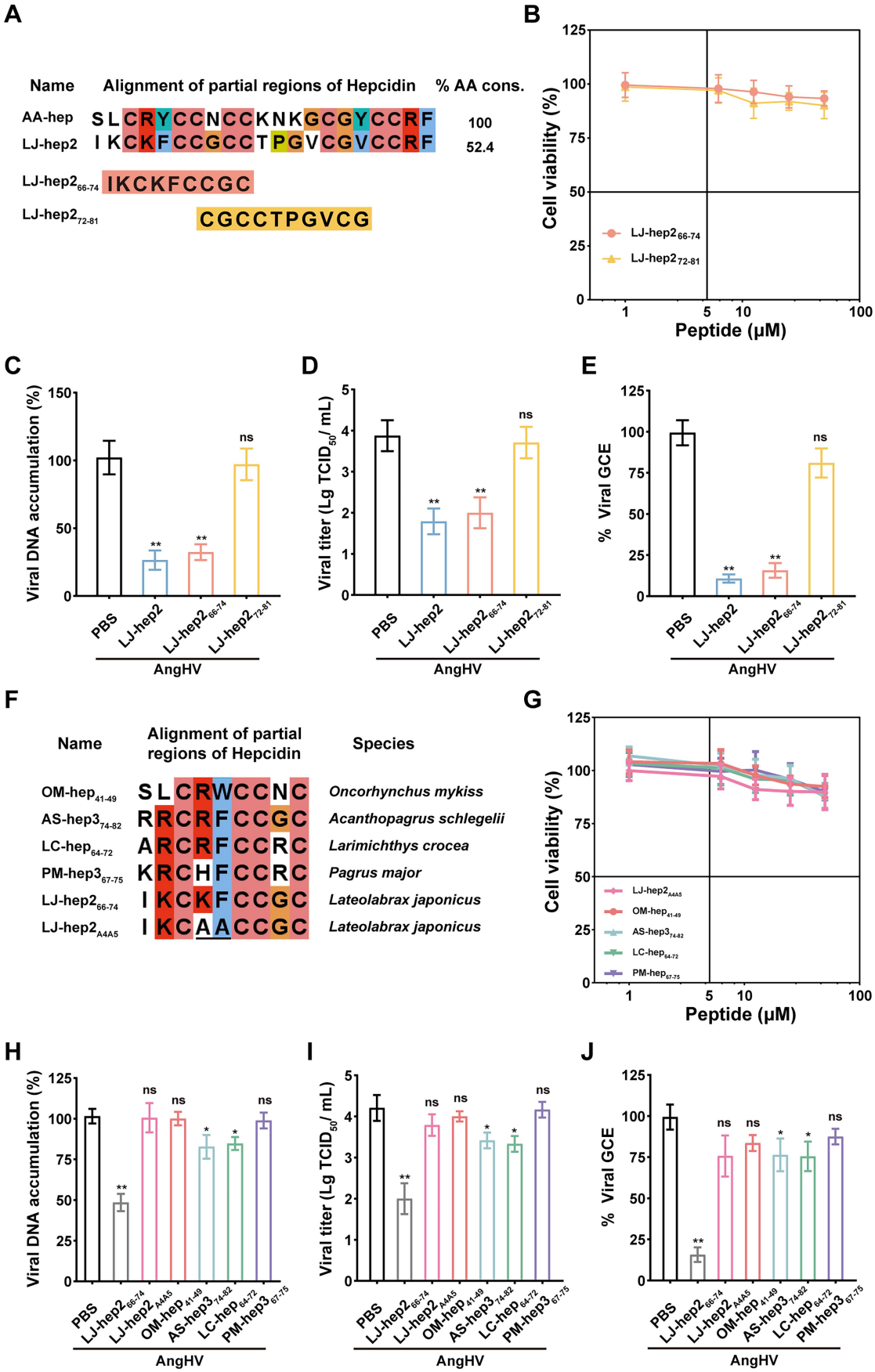

Figure 5. Antiviral activity of the truncated fragment derived from LJ-hep2 *in vitro*.

while OM-hep$_{41–49}$ and PM-hep3$_{67–75}$ had no obvious inhibitory effect on AngHV (Figure 5(H–J)). These findings confirm that the N-terminal regions of LJ-hep2, particularly Lys-4 and Phe-5, are key amino acids contributing to its effective antiviral activity.

LJ-hep2 inhibits AngHV infection in vivo

Due to the potent anti-AngHV activity of LJ-hep2 *in vitro*, we further evaluated its anti-AngHV activity *in vivo*. First, the stability of LJ-hep2 in the aquatic environment was tested. As shown in Figure 6(A), LJ-hep2 could maintain 55.5% of its antiviral activity in aquatic water for 24 h, suggesting it was relatively stable in eel culture water. Moreover, when LJ-hep2 was present at concentrations ≤1 mg/L, it did not cause eel death within 5 days (Figure 6(B)). To determine the viral titers used *in vivo*, we measured the infection rate of eels at different viral titers. The results showed that the semi-logarithm regression line "$y = 23.33x + 14.67$, $R^2 = 0.97$" between the infection rate and AngHV dose was strongly correlated (Figure 6(C)). The 50% infection dose (ID_{50}) of AngHV was calculated to be $10^{1.5}$ $TCID_{50}$/mL. To evaluate the protective effect of LJ-hep2 against AngHV infection in eels, we designed the experiment shown in Figure 6D. The eels ($n = 21$) were infected with AngHV at ID_{50} in the presence or absence of LJ-hep2. At 72 hpi, the viral loads in the visceral tissues of the LJ-hep2-treated group were significantly lower than those of the PBS group (Figure 6(E)), and the infection rate of eels in the control group was 57.1%, whereas the infection rate of eels treated with LJ-hep2 was 33.3% (Figure 6(F)).

To evaluate the potential application value of LJ-hep2, we designed a horizontal transmission model of eels infected by AngHV (Figure 6(G)). In this model, AngHV-infected donor fish and healthy recipient fish were mixed breeding in a ratio of 1:5 and treated with/without LJ-hep2 daily for the first 3 days after mixing. After an additional 3 days of treatment, 10 recipient fish were randomly selected for viral detection, and the remaining recipient and donor fish ($n = 20$) were kept for another 15 days for survival statistics. Compared to the eels in the control (PBS) group with up to 70% infection, recipient fish in the LJ-hep2-treated group were infected with only 10% of the virus after 3 days of treatment (Figure 6(H)). At 21 dpi, the overall survival rate of fish in the LJ-hep2-treated group reached 90%, which was significantly higher than that in the PBS group (25%) (Figure 6(I)). In addition, histopathological analysis of the skin tissue confirmed that the epidermal cells of the AngHV-infected eel were partially or completely detached in the PBS group, while no obvious pathological changes were observed in the LJ-hep2-treated group (Figure 6(J)). These results suggested that LJ-hep2 reduced the horizontal transmission ability of AngHV and could be used as a therapeutic agent to protect eels from the threat of AngHV infection in aquaculture.

Discussion

Hemorrhagic disease caused by AngHV is a serious threat to farmed eels [3,48]. Vaccination would be very feasible to reduce the viral infection in eel, but the specific vaccine against AngHV has not yet been developed until now. The alternative choice is to find antiviral drugs like herbal remedies, and some antiviral drugs or herbal remedies have been applied in eel ponds during disease outbreaks; however, the antiviral efficacy exerted by these antiviral products is not satisfactory [49].

Antiviral agents can be divided into two groups based on their inhibitory mechanisms: (1) inhibitors that directly target the virus and (2) inhibitors that target host cell factors [50]. Virus-targeted antiviral agents concentrate on inhibiting key transcription and replication enzymes [51,52] or directly inactivating viral structural proteins [53]. However, host-targeted antivirals mainly focus on certain critical cytokines, such as interferons [54,55] and Cyclophilin inhibitors [56]. Unfortunately, the emergence of viral drug resistance [57,58], coupled with co-infections and the re-emergence of viruses [59,60], has necessitated the

(A) Schematic of the truncated fragment derived from LJ-hep2. (B) EO cells treated with LJ-hep2$_{66–74}$, and LJ-hep2$_{72–81}$ alone underwent MTS analysis to assess cell viability at 48 h. (C and D) AngHV (0.1 MOI) was preincubated with LJ-hep2/LJ-hep2$_{66–74}$/LJ-hep2$_{72–81}$ (12.5 μM) or PBS at 27°C for 1 h and the mixture was then added to EO cells. The intracellular AngHV DNA level (48 hpi) and the viral titer were measured. (E) MNase digestion experiment was used to detect the genomic DNA unreleased by AngHV (10^7 copies) treated with LJ-hep2/LJ-hep2$_{66–74}$/LJ-hep2$_{72–81}$ (12.5 μM). (F) Alignment of partial regions of hepcidin from different species and the mutant. (G) EO cells treated with LJ-hep2$_{A4A5}$, OM-hep$_{41–49}$, AS-hep3$_{74–82}$, LC-hep$_{64–72}$ and PM-hep3$_{67–75}$ alone underwent MTS analysis at 48 h. (H and I) AngHV (0.1 MOI) was preincubated with LJ-hep2$_{66–74}$/LJ-hep2$_{A4A5}$/OM-hep$_{41–49}$/AS-hep3$_{74–82}$/LC-hep$_{64–72}$/PM-hep3$_{67–75}$ (12.5 μM) or PBS for 1 h and the mixture was then added to EO cells. The viral copies (48 hpi) and the viral titer were measured. (J) MNase digestion experiment was used to detect the genomic DNA unreleased by AngHV (10^7 copies) treated with LJ-hep2$_{66–74}$/LJ-hep2$_{A4A5}$/OM-hep$_{41–49}$/AS-hep3$_{74–82}$/LC-hep$_{64–72}$/PM-hep3$_{67–75}$ (12.5 μM). The data were representative of three independent experiments and expressed as mean ± SD ($n = 3$). ns: not significant, *: $p < 0.05$, **: $p < 0.01$.

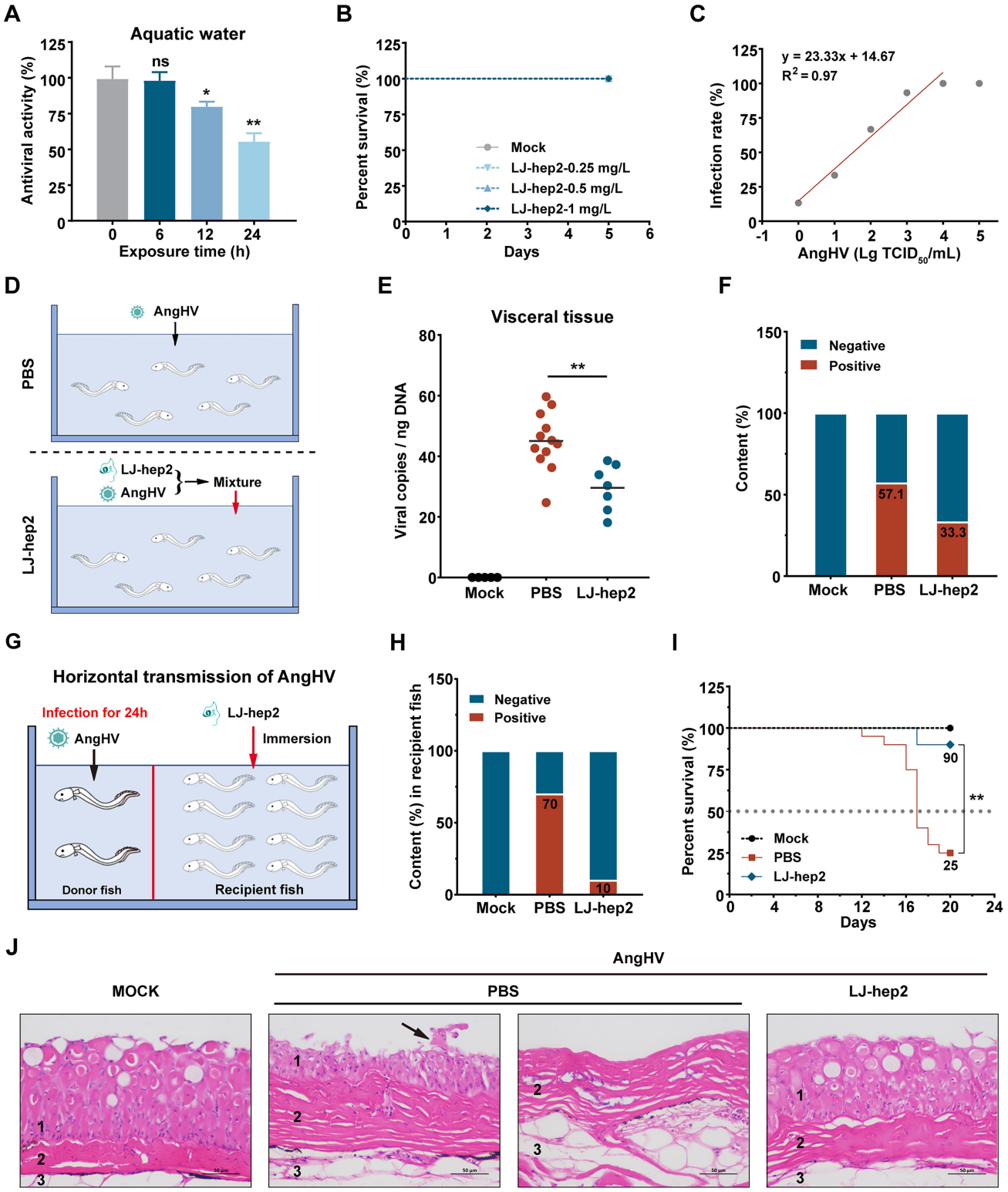

Figure 6. LJ-hep2 inhibits AngHV infection *in vivo*.

(A) The related stability of LJ-hep2 in aquatic water at 27°C. LJ-hep2 (12.5 μM) was added to aquatic water and placed at 27°C for multiple time points (6 h, 12 h, and 24 h). Subsequently, AngHV (0.1 MOI) was mixed with each sample (including 12.5 μM) and added to EO cells. At 48 hpi, the viral copies were determined by a qPCR assay. Each value is represented as the mean ± SD normalized to values for no treatment. (B) Survival rates of *Anguilla rostrata* soaked with LJ-hep2 (0.25, 0.5, and 1 mg/L) for five days ($n = 10$). (C) Correlation of infection rate of eels and infected AngHV doses (10^{0-5} $TCID_{50}$/mL; $n = 15$). The broken line indicates a regression line. (D) The schematic representation of antiviral experiment of LJ-hep2 in eels. (E and F) The eels were infected with AngHV ($10^{1.5}$ $TCID_{50}$/mL) in the presence or absence of LJ-hep2 (1 mg/L). The AngHV copies in visceral tissues and numbers of infected eels were detected via qPCR at 72 hpi ($n = 21$). (G) Schematic of the experimental design. Inhibition of the LJ-hep2 (0.5 mg/L) on horizontal transmission of AngHV. (H) Numbers of

search for new molecules with antiviral properties. Consequently, the use of AMPs has emerged as an intriguing alternative approach. Our research group has focused on the screening and identification of novel AMPs from marine animals [61–64]. In a previous study, the peptide Sparamosin$_{26–54}$, isolated from *Scylla paramamosain*, not only had antibacterial and antifungal effects but also exhibited antiviral effects against white spot syndrome virus (WSSV) [65]. Currently, only a limited number of AMPs have antiviral properties [66,67], so there is an urgent need to explore the potential for more commercially available antiviral agents. In this study, a hepcidin homolog LJ-hep2 identified from *L. japonicus* in our earlier study [68] was shown to have potent antiviral activity against AngHV. This finding would give a hint that for every known AMP, in addition to being an immune component, it may function far beyond what has been discovered so far.

Hepcidin is initially discovered in mammals [69–71], and reported later in fish [72]. Unlike mammals, which typically have only one hepcidin gene (with the mouse being an exception [73]), many fish species possess multiple hepcidin variants [74,75]. Fish hepcidins are synthesized in various tissues, including the liver, spleen, and kidney [76,77]. As an AMP, the antibacterial activity of hepcidin is well-documented [28,64,78,79], but information on its effects on the pathogenesis of viral infections is relatively limited. Previous studies report that hepcidins may inhibit viral infections in fish by modulating immune responses through Mx proteins, IFN-like, and TNF [28,29]. However, our study did not obtain similar results. LJ-hep2 did not induce cellular responses, and LJ-hep2-treated viruses triggered significantly lower immune responses than untreated viruses. This suggested that the antiviral activity of LJ-hep2 is more likely to act directly on the virus. This conclusion was supported by the time-of-addition assay, in which LJ-hep2 significantly inhibited viral replication and reduced viral entry in the viral pre-treatment manner only. Furthermore, LJ-hep2 showed the ability to inactivate the virions. Therefore, we speculated that different hepcidins may have distinct antiviral mechanisms against different viruses.

Direct interaction of antiviral factors with viral proteins has been considered the general antiviral mechanism for enveloped viruses. In our study, the results of molecular docking and pull-down assay showed that LJ-hep2 exhibited the strongest binding affinity to ORF51 compared to other envelope proteins of AngHV. Meanwhile, compared with AA-hep, a peptide that possesses a lower binding ability to ORF51, LJ-hep2 binds AngHV more effectively and exhibits stronger antiviral activity against AngHV. These findings indicated that ORF51 May be a key target of LJ-hep2 against AngHV. ORF51 is one of the most abundant proteins in AngHV envelope and plays an important role in the process of viral infection [37]. Its interaction with LJ-hep2 May bring permanent and sustained viral damage. The electron microscope observations and DNase digestion assays further confirmed our speculations. Compared with AA-hep, LJ-hep2 could disrupt the integrity of the AngHV virions more potently, resulting in the release of viral genomic DNA from the interior of virions. These results suggested that ORF51 might be a pivotal target for future screening of anti-AngHV drugs. Similar functions of AMPs have been reported. For example, the AMP brevinin-2GHk (BR2GK) was found to cause leakage of the viral genome, leading to the direct inactivation of Zika virus (ZIKV) [80]. Yodha, an amphibian host defense peptide, has been reported to have strong viricidal activity against ZIKV and all four dengue virus serotypes [81]. The precise mechanisms by which these natural AMPs antiviral functions remain largely undetermined require further investigation. In addition, Yu et al. also found that the stem region of the ZIKV envelope protein (Z2) could interact with the ZIKV E protein and induce the release of the viral genome [53]. This class of designed peptides, engineered to target critical regions of viral proteins, exhibits relatively specific effects. However, many settings need to be considered, such as the topology, amino acid composition, and charge [82], and the effectiveness of artificial AMP design strategies needs to be further investigated [83].

Through the use of truncated peptides for antiviral studies, we found that the N-terminus of LJ-hep2 was a key region for its antiviral activity in which LJ-hep2$_{66–74}$ exhibited similar antiviral efficacy as the full-length LJ-hep2. Software predictions suggested that the binding sites of LJ-hep2 to the ORF51 protein are predominantly located within the N-terminal region of LJ-hep2. Notably, the fourth and fifth amino acids in LJ-hep2 markedly diverge from those of hepcidin in various other species. Our

recipient fish infected with AngHV were determined by qPCR at 72 hpi ($n = 10$). (I) Survivorship curves of the donor and recipient eels ($n = 20$). (J) Representative micrographs of the histological alterations in the skin of eels. The regular structure of skin from the mock group showed a stratified granular epithelium (1), a compact dermis (2), and a part of and hypodermis (3). The black arrow indicated the exfoliation of epidermal cells. ns: not significant, *: $p < 0.05$, **: $p < 0.01$.

antiviral experiments indicated that hepcidins from those other species exhibited minimal or no anti-AngHV activity. Further investigations revealed that the mutant peptide LJ-hep2$_{A4A5}$, which lost the crucial amino acids, was deprived of its anti-AngHV activity, highlighting the importance of the fourth and fifth residues in LJ-hep2. Upon analyzing the binding sites, we found that LJ-hep2 interacts with the intermediate transmembrane region of ORF51, whereas AA-hep binds primarily to the intracellular region of ORF51. Both LJ-hep2 and AA-hep are cationic and hydrophobic, but LJ-hep2 exhibits relatively higher hydrophobicity. Hydrophobicity is essential for the insertion and penetration of bilayers because hydrophobic amino acids can interact with the membrane core [84–86]. Additionally, hydrophobic peptides can interact with the transmembrane segments of viral proteins, leading to critical conformational changes that result in the destabilization of the viral structure [87]. This suggests that the antiviral mechanism of LJ-hep2 May involve its insertion into the viral membrane through its high hydrophobicity, allowing it to bind to specific amino acid sites in the transmembrane region of ORF51 (Figure 7 left). In contrast, AA-hep may only be able to partially disrupt the viral membrane and penetrate the virion interior, resulting in a lower antiviral activity compared to LJ-hep2 (Figure 7 right). Overall, understanding the mechanism of LJ-hep2 provides a strong foundation for its potential development as an antiviral agent for the treatment of AngHV infection.

The medicinal metabolism of antiviral drugs in fish is progressively accelerated, as they must be re-injected periodically to eliminate the viral threat, which limits their use in aquaculture [88]. Therefore, it is preferable

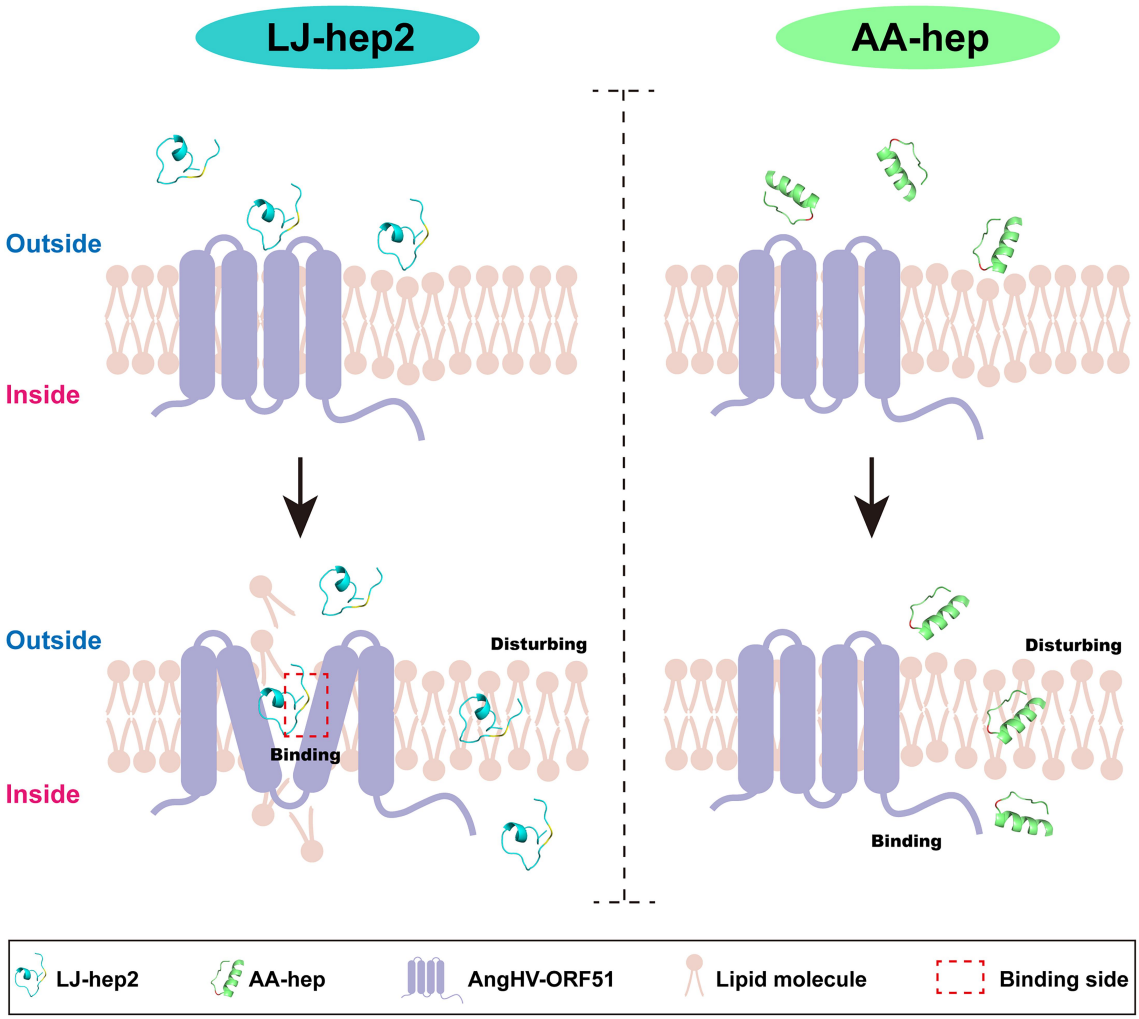

Figure 7. Schematic representation of the action of LJ-hep2 and AA-hep on the AngHV envelope.

The Effects of LJ-hep2 and AA-hep on the integrity of AngHV envelope. LJ-hep2 and AA-hep leverage their hydrophobic properties to disturb the viral membrane, inducing structural instability in the virus and ultimately leading to its inactivation. Notably, LJ-hep2 exhibits higher hydrophobicity, potentially enabling it to squeeze out lipids near the transmembrane region of ORF51 and bind to the corresponding amino acid sites. This heightened interaction between LJ-hep2 and ORF51 results in more profound destruction of the viral structure.

to evaluate the efficacy of the peptides on diseased eels using medicated baths [49]. In this study, we found that the presence of LJ-hep2 (at a dose of 1 mg/L) significantly reduced viral infection in eels exposed to AngHV. According to the epidemiological investigation, hemorrhagic disease occurs only once in the breeding cycle, and rehabilitated eels are no longer susceptible to AngHV [89]. To assess the anti-AngHV effectiveness of the peptide in eels, a horizontally transmitted infection assay was performed. Notably, LJ-hep2 could reduce viral infection and eliminate skin lesions in eels by inhibiting viral horizontal transmission, which is expected to be developed as a novel anti-AngHV agent.

As widely recognized, hepcidin acts as a major iron-regulating hormone, playing a crucial role in iron regulation and systemic iron homeostasis [90–92]. Hepcidin regulates iron uptake and efflux by directly binding to the iron exporter ferroportin, leading to the degradation of this transporter [90]. Iron is a nutrient required by pathogens, and the deprivation of iron serves as an innate immune mechanism against pathogen invasion [93]. Previous studies in mammals have shown that hepcidin protects against Hepatitis B Virus (HBV), Hepatitis C Virus (HCV), and Human Immunodeficiency Virus (HIV) infection by sequestering iron from pathogens [90–92,94–96]. Whether iron is required for AngHV infection and whether hepcidin inhibits AngHV infection through iron regulation remains to be further investigated.

In conclusion, we evaluated the potential activity of four marine-derived AMPs against AngHV, and a hepcidin homolog LJ-hep2 from Japanese seabass *L. japonicus* [23] was identified as a promising antiviral agent that showed inhibition on AngHV infection in eel farming. *In vitro*, LJ-hep2 exhibited the ability to bind to virions, thereby hindering the entry of AngHV into cells and diminishing viral replication. *In vivo*, LJ-hep2 reduced viral accumulation in tissues and inhibited horizontal transmission of AngHV, including lowering infection rates, alleviating skin lesions, and improving survival in recipient fish. Additionally, LJ-hep2 was found to interact with AngHV envelope protein ORF51 and directly disrupted the viral structure. Based on our findings, we proposed the differences in the anti-AngHV mechanisms of LJ-hep2 and AA-hep. LJ-hep2 May enhance its antiviral activity by leveraging its hydrophobicity to disrupt viral lipid molecules and bind to the amino acids in the transmembrane region of ORF51, thereby altering membrane conformation. Unlike LJ-hep2, AA-hep may primarily affect viral membrane stability through its physical properties, such as hydrophobicity. Moreover, the antiviral properties of LJ-hep2, coupled with its safety profile and ease of degradation, advocate the use of LJ-hep2 as a promising therapeutic candidate for the treatment of eel AngHV disease. Particularly, the relatively easy availability of LJ-hep2 suggests that it has the potential to be an option for the treatment of AngHV infections in the absence of an approved vaccine.

Acknowledgements

We are grateful to the Institute of Biotechnology, Fujian Academy of Agricultural Sciences (Fuzhou, China), particularly to Jin-Xian Yang for his guidance in AngHV preparation and eel cell culture, and to Qiang Chen for his assistance in American eel farming before animal experiments. Special thanks to the laboratory engineers Ming Xiong, Hui Peng, Zhiyong Lin, Huiyun Chen, and Hua Hao from Xiamen University, Xiamen, China, for providing additional technical support.

Author contributions

CRediT: **Yingyi Duan:** Data curation, Formal analysis, Investigation, Methodology, Software, Visualization, Writing – original draft; **Jun-Qing Ge:** Project administration, Resources, Writing – review & editing; **Xin-Zhan Meng:** Data curation, Formal analysis, Methodology, Software, Validation, Writing – review & editing; **Fangyi Chen:** Conceptualization, Funding acquisition, Project administration, Resources, Supervision, Writing – review & editing; **Ke-Jian Wang:** Conceptualization, Funding acquisition, Project administration, Resources, Supervision, Writing – review & editing.

Funding

This work was supported by grant [42376089] from the National Natural Science Foundation of China; grant [2025N5001] from the Fujian Province Industry-Academia Collaboration Project; grant [XTCXGC2021013] from the "5511" Collaborative Innovation Project of Fujian Academy of Agricultural Sciences; grant [FJHYF-L-2025–13] from Fujian Ocean and Fisheries Bureau; grant [22CZP002HJ08] from Xiamen Ocean Development Bureau, and grant [Z20220743] from Pingtan Research Institute of Xiamen University.

Disclosure statement

No potential conflict of interest was reported by the author(s).

Data availability statement

The raw data supporting the findings of this study are openly available in Figshare at https://doi.org/10.6084/m9.figshare.26963620.v1 [97].

Ethics statement

All experiments were conducted by standard biosecurity and institutional safety procedures established by Xiamen University. Animal experiments were approved by the Laboratory Animal Management and Ethics Committee of Xiamen University and were performed following the European Union guidelines for handling laboratory animals (2010/63/EU).

ORCID

Ke-Jian Wang http://orcid.org/0000-0003-0764-9956

References

[1] Food and Agriculture Qrganization of United Nations (FAO). Fishery and aquaculture statistics. Global production by production source 1950 – 2018 (FishstatJ). Rome: FAO; 2020. Available from: https://www.fao.org/fishery/en/topic/166235

[2] van Beurden SJ, Engelsma MY, Roozenburg I, et al. Viral diseases of wild and farmed European eel *Anguilla anguilla* with particular reference to the Netherlands. Dis Aquat Organ. 2012;101(1):69–86. doi: 10.3354/dao02501

[3] Ginneken V, Haenen OLM, Coldenhoff K, et al. Presence of eel viruses in eel species from various geographic regions. Bull Eur Ass Fish Pathol. 2004;24:268–272.

[4] McConville J, Fringuelli E, Evans D, et al. First examination of the Lough Neagh European eel (*Anguilla anguilla*) population for eel virus European, eel virus European X and Anguillid herpesvirus-1 infection by employing novel molecular techniques. J Fish Dis. 2018;41(12):1783–1791. doi: 10.1111/jfd.12885

[5] van Beurden SJ, Bossers A, Voorbergen-Laarman MHA, et al. Complete genome sequence and taxonomic position of Anguillid herpesvirus 1. J Gen Virol. 2010;91(4):880–887. doi: 10.1099/vir.0.016261-0

[6] European Food Safety Authority (EFSA). Animal welfare aspects of husbandry systems for farmed Atlantic salmon - scientific opinion of the panel on animal health and welfare. ESFA J. 2008;6(7):736. doi: 10.2903/j.efsa.2008.736

[7] van Nieuwstadt AP, Dijkstra SG, Haenen OL. Persistence of herpesvirus of eel herpesvirus anguillae in farmed European eel *Anguilla anguilla*. Dis Aquat Organ. 2001;45(2):103–107. doi: 10.3354/dao045103

[8] Yang JX, Chen Q, Li YY, et al. Hemorrhagic gill rot of *Anguilla anguilla* and its comprehensive control. Aquacult (China). 2021;42(2):76–77.

[9] Ge JQ, Yang JX, Gong H, et al. Isolation and identification of a herpesvirus from cultured European eels *anguilla anguilla* in China. J Fish China. 2014;38 (9):1579–1583.

[10] Li YY, Yang JX, Chen X, et al. Proteomic profiling skin mucus of European eel *Anguilla anguilla* infected with Anguillid Herpesvirus. Int J Mol Sci. 2022;23 (19):11283. doi: 10.3390/ijms231911283

[11] Fan HP, Yang M, Zhang JL, et al. Prevalence of anguillid herpesvirus 1 and control techniques. Sci Fish Farming (China). 2019;8:46–48.

[12] Schulz P, Deperasińska I, E K-Ł, et al. Immunosuppressive influence of Anguillid herpesvirus-1 (AngHV-1) infection on cellular defense mechanisms in European eel (*Anguilla anguilla*). Pol J Vet Sci. 2019;22(4):785–787.

[13] Vilas Boas LCP, Campos ML, Berlanda RLA, et al. Antiviral peptides as promising therapeutic drugs. Cell Mol Life Sci. 2019;76(18):3525–3542. doi: 10.1007/s00018-019-03138-w

[14] Hemshekhar M, Anaparti V, Mookherjee N. Functions of cationic host defense peptides in immunity. Pharmaceuticals (Basel). 2016;9(3):40. doi: 10.3390/ph9030040

[15] Hilchie AL, Wuerth K, Hancock REW. Immune modulation by multifaceted cationic host defense (antimicrobial) peptides. Nat Chem Biol. 2013;9(12):761–768. doi: 10.1038/nchembio.1393

[16] Mansour SC, Pena OM, Hancock REW. Host defense peptides: front-line immunomodulators. Trends Immunol. 2014;35(9):443–450. doi: 10.1016/j.it.2014.07.004

[17] Sable R, Parajuli P, Jois S. Peptides, peptidomimetics, and polypeptides from marine sources: a wealth of natural sources for pharmaceutical applications. Mar Drugs. 2017;15(4):124. doi: 10.3390/md15040124

[18] Macedo MWFS, NBd C, Carneiro JA, et al. Marine organisms as a rich source of biologically active peptides. Front Mar Sci. 2021;8:667764.

[19] Ovchinnikova TV. Marine peptides: structure, bioactivities, and a new hope for therapeutic application. Mar Drugs. 2021;19(8):407. doi: 10.3390/md19080407

[20] Stevenson CL. Advances in peptide pharmaceuticals. Curr Pharm Biotechnol. 2009;10(1):122–137. doi: 10.2174/138920109787048634

[21] Mahlapuu M, Björn C, Ekblom J. Antimicrobial peptides as therapeutic agents: opportunities and challenges. Crit Rev Biotechnol. 2020;40(7):978–992. doi: 10.1080/07388551.2020.1796576

[22] Mulder K, Lima LA, Miranda V, et al. Current scenario of peptide-based drugs: the key roles of cationic antitumor and antiviral peptides. Front Microbiol. 2013;4:321. doi: 10.3389/fmicb.2013.00321

[23] Gong R, An Z, Zhang W, et al. The antimicrobial peptide LJ-hep2 from *Lateolabrax japonicus* exerting activities against multiple pathogenic bacteria and immune protection *in vivo*. Mar Drugs. 2022;20 (10):651. doi: 10.3390/md20100651

[24] Zhou Y, Meng X, Chen F, et al. Newly discovered antimicrobial peptide scyampcin$_{44–63}$ from *Scylla paramamosain* exhibits a multitargeted candidacidal mechanism *in vitro* and is effective in a murine model of vaginal candidiasis. Antimicrob Agents Chemother. 2023;67(6): e0002223. doi: 10.1128/aac.00022-23

[25] Bo J, Yang Y, Zheng R, et al. Antimicrobial activity and mechanisms of multiple antimicrobial peptides isolated from rockfish *Sebastiscus marmoratus*. Fish Shellfish Immunol. 2019;93:1007–1017. doi: 10.1016/j.fsi.2019.08.054

[26] Hu Y, Kurobe T, Liu X, et al. Hamp type-1 promotes antimicrobial defense via direct microbial killing and regulating iron metabolism in grass carp (*Ctenopharyngodon idella*). Biomolecules. 2020;10 (6):825. doi: 10.3390/biom10060825

[27] Li H, Zhang F, Guo H, et al. Molecular characterization of hepcidin gene in common carp (*Cyprinus carpio* L.) and its expression pattern responding to bacterial challenge. Fish Shellfish Immunol. 2013;35(3):1030–1038. doi: 10.1016/j.fsi.2013.07.001

[28] Wang YD, Kung CW, Chi SC, et al. Inactivation of nervous necrosis virus infecting grouper (*Epinephelus coioides*) by epinecidin-1 and hepcidin 1–5 antimicrobial peptides, and downregulation of Mx2 and Mx3 gene expressions. Fish Shellfish Immunol. 2010;28(1):113–120.

[29] Rajanbabu V, Chen JY. Antiviral function of tilapia hepcidin 1–5 and its modulation of immune-related gene expressions against infectious pancreatic necrosis virus (IPNV) in Chinook salmon embryo (CHSE)-214 cells. Fish Shellfish Immunol. 2011;30(1):39–44.

[30] Reed LJ, Muench H. A simple method of estimating fifty percent endpoints. Am J Epidemiol. 1938;27(3):493–497. doi: 10.1093/oxfordjournals.aje.a118408

[31] Xu XQ, Xu T, Ji W, et al. Herpes simplex virus 1-induced ferroptosis contributes to viral encephalitis. mBio. 2023;14(1):e0237022. doi: 10.1128/mbio.02370-22

[32] Li YY, Yang JX, Chen X, et al. Establishment and application of SYBR green I real-time fluorescence quantitative PCR for detection of Anguillid herpesvirus. J Fish China. 2021;45(5):769–777.

[33] Chen X, Yang JX, Chen H, et al. Identification, expression, and characterization analysis immunogenic protein ORF36 of Anguillid herpesvirus. J Agric Biotechnol (China). 2023;31(8):1710–1718 .

[34] Li YY, Chen X, Yang JX, et al. Evaluation of housekeeping genes as references for quantitative real-time PCR analysis of European eel. Anguilla J Fish Biol. 2023;102(1):141–154.

[35] Livak KJ, Schmittgen TD. Analysis of relative gene expression data using real-time quantitative PCR and the 2(-delta delta C(T)) method. Methods. 2001;25(4):402–408. doi: 10.1006/meth.2001.1262

[36] Pu J, He X, Xu W, et al. The analogs of furanyl methylidene rhodanine exhibit broad-spectrum inhibitory and inactivating activities against enveloped viruses, including SARS-CoV-2 and its variants. Viruses. 2022;14(3):489. doi: 10.3390/v14030489

[37] van Beurden SJ, Leroy B, Wattiez R, et al. Identification and localization of the structural proteins of anguillid herpesvirus 1. Vet Res. 2011;42(1):105. doi: 10.1186/1297-9716-42-105

[38] Lok SM, Costin JM, Hrobowski YM, et al. Release of dengue virus genome induced by a peptide inhibitor. PLOS ONE. 2012;7(11):e50995. doi: 10.1371/journal.pone.0050995

[39] Zhou P, Jin B, Li H, et al. HPEPDOCK: a web server for blind peptide–protein docking based on a hierarchical algorithm. Nucleic Acids Res. 2018;46(W1):W443–W450. doi: 10.1093/nar/gky357

[40] Seeliger D, de Groot BL. Ligand docking and binding site analysis with PyMOL and AutoDock/Vina. J Comput Aided Mol Des. 2010;24(5):417–422. doi: 10.1007/s10822-010-9352-6

[41] Hangalapura BN, Zwart R, Engelsma MY, et al. Pathogenesis of herpesvirus anguillae (HVA) in juvenile European eel *Anguilla anguilla* after infection by bath immersion. Dis Aquat Organ. 2007;78(1):13–22. doi: 10.3354/dao01849

[42] Canei J, Trupia A, Nonclercq D. Cytological analysis of integumentary and muscular adaptations in three sand-dwelling marine teleosts, *Ammodytes tobianus* (Ammodytidae), *Gorgasia preclara* (Congridae) and *Heteroconger hassi* (Congridae) (Teleostei; Actinopterygii). J Fish Biol. 2020;97(4):1097–1112. doi: 10.1111/jfb.14472

[43] Meng XZ, Shen YB, Wang ST, et al. Complement component 3 (C3): an important role in grass carp (*Ctenopharyngodon idella*) experimentally exposed to *aeromonas hydrophila*. Fish Shellfish Immunol. 2019;88:189–197. doi: 10.1016/j.fsi.2019.02.061

[44] Falco A, Chico V, Marroqui L, et al. Expression and antiviral activity of a β-defensin-like peptide identified in the rainbow trout (*Oncorhynchus mykiss*) EST sequences. Mol Immunol. 2008;45(3):757–765. doi: 10.1016/j.molimm.2007.06.358

[45] Fang Y, Wang C, Wang C, et al. Antiviral peptides targeting the helicase activity of enterovirus nonstructural protein 2C. J Virol. 2021;95(12):e02324–20. doi: 10.1128/JVI.02324-20

[46] Nie C, Stadtmüller M, Parshad B, et al. Heteromultivalent topology-matched nanostructures as potent and broad-spectrum influenza A virus inhibitors. Sci Adv. 2021;7(1):eabd3803. doi: 10.1126/sciadv.abd3803

[47] Xiao B, Fu Q, Niu S, et al. Penaeidins restrict white spot syndrome virus infection by antagonizing the envelope proteins to block viral entry. Emerg Microbes Infect. 2020;9(1):390–412. doi: 10.1080/22221751.2020.1729068

[48] Haenen OLM, Dijkstra SG, Tulden P, et al. Herpesvirus anguillae (HVA) isolations from disease outbreaks in cultured European eel, *Anguilla anguilla* in the Netherlands since 1996. Bull Eur Ass Fish Pathol. 2002;22:247–257.

[49] Fan HP, Zhong QF, Yang H, et al. Efficacy of an antivirus drug on treating anguillid herpesvirus disease of cultured American eels. Chin Agric Sci Bull (China). 2021;37(5):124–129.

[50] Lou Z, Sun Y, Rao Z. Current progress in antiviral strategies. Trends Pharmacol Sci. 2014;35(2):86–102. doi: 10.1016/j.tips.2013.11.006

[51] Kiser JJ, Flexner C. Direct-acting antiviral agents for hepatitis C virus infection. Annu Rev Pharmacol Toxicol. 2013;53(1):427–449. doi: 10.1146/annurev-pharmtox-011112-140254

[52] McDonald CK, Kuritzkes DR. Human immunodeficiency virus type 1 protease inhibitors. Arch Intern Med. 1997;157(9):951–959. doi: 10.1001/archinte.1997.00440300037003

[53] Yu Y, Deng YQ, Zou P, et al. A peptide-based viral inactivator inhibits Zika virus infection in pregnant mice and fetuses. Nat Commun. 2017;8(1):15672. doi: 10.1038/ncomms15672

[54] Lin FC, Young HA. Interferons: success in anti-viral immunotherapy. Cytokine Growth Factor Rev. 2014;25(4):369–376. doi: 10.1016/j.cytogfr.2014.07.015

[55] Raziky EM, Fathalah WF, El-Akel WA, et al. The effect of peginterferon alpha-2b in treatment of naive chronic HCV genotype-4 patients: a single centre Egyptian

study. Hepat Mon. 2013;13(5):e10069. doi: 10.5812/hepatmon.10069

[56] Liu X, Zhao Z, Liu W. Insights into the roles of cyclophilin A during influenza virus infection. Viruses. 2013;5(1):182–191. doi: 10.3390/v5010182

[57] Duraffour S, Andrei G, Topalis D, et al. Mutations conferring resistance to viral DNA polymerase inhibitors in camelpox virus give different drug-susceptibility profiles in vaccinia virus. J Virol. 2012;86(13):7310–7325. doi: 10.1128/JVI.00355-12

[58] Musiime V, Kaudha E, Kayiwa J, et al. Antiretroviral drug resistance profiles and response to second-line therapy among HIV type 1-infected Ugandan children. AIDS Res Hum Retroviruses. 2013;29(3):449–455. doi: 10.1089/aid.2012.0283

[59] Hui DSC, Lee N, Chan PKS. A clinical approach to the threat of emerging influenza viruses in the Asia-Pacific region. Respirology. 2017;22(7):1300–1312.

[60] Deming P, McNicholl IR. Coinfection with human immunodeficiency virus and hepatitis C virus: challenges and therapeutic advances. Insights from the Society of Infectious Diseases Pharmacists. Pharmacotherapy. 2011;31(4):357–368. doi: 10.1592/phco.31.4.357

[61] Bai Y, Zhang W, Zheng W, et al. A 14-amino acid cationic peptide bolespleenin$_{(334–347)}$ from the marine fish mudskipper *Boleophthalmus pectinirostris* exhibiting potent antimicrobial activity and therapeutic potential. Biochem Pharmacol. 2024;226:116344.

[62] Wang KJ, Huang WS, Yang M, et al. A male-specific expression gene, encodes a novel anionic antimicrobial peptide, scygonadin, in *Scylla serrata*. Mol Immunol. 2007;44(8):1961–1968. doi: 10.1016/j.molimm.2006.09.036

[63] Wang KJ, Cai JJ, Cai L, et al. Cloning and expression of a hepcidin gene from a marine fish (*Pseudosciaena crocea*) and the antimicrobial activity of its synthetic peptide. Peptides. 2009;30(4):638–646. doi: 10.1016/j.peptides.2008.12.014

[64] Yang M, Chen B, Cai JJ, et al. Molecular characterization of hepcidin AS-hepc2 and AS-hepc6 in black porgy (*Acanthopagrus schlegelii*): expression pattern responded to bacterial challenge and *in vitro* antimicrobial activity. Comp Biochem Physiol B Biochem Mol Biol. 2011;158(2):155–163. doi: 10.1016/j.cbpb.2010.11.003

[65] Meng XZ, Duan Y, Bai Y, et al. The antimicrobial peptide sparamosin$_{26–54}$ exhibits antiviral activity against three aquatic enveloped viruses through lipid-binding-mediated virus lysis. Aquaculture. 2024;592:741160. doi: 10.1016/j.aquaculture.2024.741160

[66] Liu HP, Chen RY, Zhang QX, et al. Characterization of two isoforms of antiliopolysacchride factors (sp-ALFs) from the mud crab *Scylla paramamosain*. Fish Shellfish Immunol. 2012;33(1):1–10. doi: 10.1016/j.fsi.2012.03.014

[67] Peng H, Liu HP, Chen B, et al. Optimized production of scygonadin in Pichia pastoris and analysis of its antimicrobial and antiviral activities. Protein Expr Purif. 2012;82(1):37–44. doi: 10.1016/j.pep.2011.11.008

[68] Ren HL, Wang KJ, Zhou HL, et al. Cloning and organisation analysis of a hepcidin-like gene and cDNA from Japan Sea Bass. Fish Shellfish Immunol. 2006;21(3):221–227. doi: 10.1016/j.fsi.2005.10.011

[69] Krause A, Neitz S, Mägert H-J, et al. Leap-1, a novel highly disulfide-bonded human peptide, exhibits antimicrobial activity. FEBS Lett. 2000;480(2–3):147–150. doi: 10.1016/S0014-5793(00)01920-7

[70] Park CH, Valore EV, Waring AJ, et al. Hepcidin, a urinary antimicrobial peptide synthesized in the liver *. J Biol Chem. 2001;276(11):7806–7810. doi: 10.1074/jbc.M008922200

[71] Pigeon C, Ilyin G, Courselaud B, et al. A new mouse liver-specific gene, encoding a protein homologous to human antimicrobial peptide hepcidin, is overexpressed during iron overload. J Biol Chem. 2001;276(11):7811–7819. doi: 10.1074/jbc.M008923200

[72] Shike H, Lauth X, Westerman ME, et al. Bass hepcidin is a novel antimicrobial peptide induced by bacterial challenge. Eur J Biochem. 2002;269(8):2232–2237. doi: 10.1046/j.1432-1033.2002.02881.x

[73] Ilyin G, Courselaud B, Troadec MB, et al. Comparative analysis of mouse hepcidin 1 and 2 genes: evidence for different patterns of expression and co-inducibility during iron overload. FEBS Lett. 2003;542(1–3):22–26.

[74] Hilton KB, Lambert LA. Molecular evolution and characterization of hepcidin gene products in vertebrates. Gene. 2008;415(1–2):40–48. doi: 10.1016/j.gene.2008.02.016

[75] Masso-Silva JA, Diamond G. Antimicrobial peptides from fish. Pharmaceuticals (Basel). 2014;7(3):265–310. doi: 10.3390/ph7030265

[76] Asmamaw B. Hepcidin and its roles in fishes. J Zool Stud. 2016;3:1–10.

[77] Yang M, Wang KJ, Chen JH, et al. Genomic organization and tissue-specific expression analysis of hepcidin-like genes from black porgy (*Acanthopagrus schlegelii* B.). Fish Shellfish Immunol. 2007;23(5):1060–1071.

[78] Rodrigues PNS, Vázquez-Dorado S, Neves JV, et al. Dual function of fish hepcidin: response to experimental iron overload and bacterial infection in sea bass (*Dicentrarchus labrax*). Dev Comp Immunol. 2006;30(12):1156–1167. doi: 10.1016/j.dci.2006.02.005

[79] Zhou JG, Wei JG, Xu D, et al. Molecular cloning and characterization of two novel hepcidins from orange-spotted grouper, *Epinephelus coioides*. Fish Shellfish Immunol. 2011;30(2):559–568. doi: 10.1016/j.fsi.2010.11.021

[80] Xiong W, Li J, Feng Y, et al. Brevinin-2ghk, a peptide derived from the skin of *Fejervarya limnocharis*, inhibits Zika virus infection by disrupting viral integrity. Viruses. 2021;13(12):2382. doi: 10.3390/v13122382

[81] Lee SH, Kim EH, O'neal JT, et al. The amphibian peptide yodha is virucidal for Zika and dengue viruses. Sci Rep. 2021;11(1):602. doi: 10.1038/s41598-020-80596-4

[82] Maccari G, Di Luca M, Nifosí R, et al. Antimicrobial peptides design by evolutionary multiobjective optimization. PLOS Comput Biol. 2013;9(9):e1003212. doi: 10.1371/journal.pcbi.1003212

[83] Cardoso MH, Orozco RQ, Rezende SB, et al. Computer-aided design of antimicrobial peptides: are we generating effective drug candidates? Front Microbiol. 2019;10:3097.

[84] Gallivan JP, Dougherty DA. Cation-π interactions in structural biology. Proc Natl Acad Sci U S A. 1999;96(17):9459–9464. doi: 10.1073/pnas.96.17.9459

[85] Persson S, Killian JA, Lindblom G. Molecular ordering of interfacially localized tryptophan analogs in ester-and ether-lipid bilayers studied by 2H-NMR. Biophys J. 1998;75(3):1365–1371.

[86] Qian Z, Martyna A, Hard RL, et al. Discovery and mechanism of highly efficient cyclic cell-penetrating peptides. Biochemistry. 2016;55(18):2601–2612. doi: 10.1021/acs.biochem.6b00226

[87] Hoffmann AR, Guha S, Wu E, et al. Broad-spectrum antiviral entry inhibition by interfacially active peptides. J Virol. 2020;94(23):e01682–20. doi: 10.1128/JVI.01682-20

[88] Liu L, Shan LP, Xue MY, et al. Potential application of antiviral coumarin in aquaculture against IHNV infection by reducing viral adhesion to the epithelial cell surface. Antiviral Res. 2021;195:105192. doi: 10.1016/j.antiviral.2021.105192

[89] Yang JX, Chen Q, Li YY, et al. Biological and physicochemical characteristics of Anguillid herpesvirus. J Fish China. 2020;44(9):1435–1440.

[90] Armitage AE, Eddowes LA, Gileadi U, et al. Hepcidin regulation by innate immune and infectious stimuli. Blood. 2011;118(15):4129–4139. doi: 10.1182/blood-2011-04-351957

[91] Michels K, Nemeth E, Ganz T, et al. Hepcidin and host defense against infectious diseases. PLOS Pathog. 2015;11(8):e1004998. doi: 10.1371/journal.ppat.1004998

[92] Walker A, Partridge J, Srai S, et al. Hepcidin: what every gastroenterologist should know. Gut. 2004;53(5):624–627.

[93] Cassat JE, Skaar EP. Iron in infection and immunity. Cell Host Microbe. 2013;13(5):509–519. doi: 10.1016/j.chom.2013.04.010

[94] Armitage AE, Stacey AR, Giannoulatou E, et al. Distinct patterns of hepcidin and iron regulation during HIV-1, HBV, and HCV infections. Proc Natl Acad Sci U S A. 2014;111(33):12187–12192. doi: 10.1073/pnas.1402351111

[95] Rodriguez R, Jung CL, Gabayan V, et al. Hepcidin induction by pathogens and pathogen-derived molecules is strongly dependent on interleukin-6. Infect Immun. 2014;82(2):745–752. doi: 10.1128/IAI.00983-13

[96] Wang XH, Cheng PP, Jiang F, et al. The effect of hepatitis B virus infection on hepcidin expression in hepatitis B patients. Ann Clin Lab Sci. 2013;43(2):126–134.

[97] Duan Y. A hepcidin homolog from *Lateolabrax japonicus* inhibits the infection of Anguillid herpesvirus 1 by interacting with the viral envelope protein ORF51-figure raw date. 2024. doi: 10.6084/m9.figshare.26963620.v1